Computing Deflections Using ACI CODE-318-19 and Beyond, Part 5

Proposed extension to prestressed concrete

by Peter H. Bischoff, Wassim Nasreddine, and Hani Nassif

Parts 1 to 4 of this article series[1-4] introduce and evaluate the new expression for I_e first adopted by ACI CODE-318-19[5] for calculating deflection of reinforced (nonprestressed) concrete. The revised expression for I_e is not applicable to cracked prestressed concrete members, and ACI CODE-318-19 uses the approach developed by Branson[6] for this type of member.

Work by Bischoff et al.[7] has proposed extending the ACI CODE-318-19 approach for reinforced concrete to include prestressed concrete. The proposed approach, summarized in Fig. 1, has been developed to compute immediate deflection of Class T and Class C prestressed members, which are cracked under service load (refer to ACI CODE-318, Section 24.5.2, for classification of prestressed members). In this approach, deformation from the eccentric prestressing force (computed using an effective eccentricity e_e and effective moment of inertia I_e) is subtracted from the deformation from load (computed using I_e). This is much like the procedure used to compute deflection of an uncracked prestressed member, in which e_g (the eccentricity of the prestressing force relative to the centroid of the gross [uncracked] section) and I_g are used to compute camber, and I_g is used to compute deflection due to load (but with one difference for a cracked member, as noted further on).

While the curvature of a cracked prestressed member is obtained by subtracting the effective curvature caused by the eccentric prestressing force from the curvature caused by load, direct calculation of deflection is conservatively based on net curvature[7] as demonstrated with an example later in this article. For a continuous member or members with variable eccentricity of the prestressing, it might be advantageous to compute deflection by integrating curvature. Calculating deflection directly (without integration) is also affected by the type of loading. A bonus example for a member with variable eccentricity is available in the Appendix, which can be accessed in the online version of this article at **www.concreteinternational.com**.

$$I_e = I_g \text{ and } e_e = e_g \text{ for } M_a \le \lambda_{cr} M_{cr}$$

For $M_a > \lambda_{cr} M_{cr}$

$$I_e = \frac{I_{cr}}{1-\left(\dfrac{\lambda_{cr} M_{cr}}{M_a}\right)^2 \left(1-\dfrac{I_{cr}}{I_g}\right)}$$

$$e_e = \left(\frac{\lambda_{cr} M_{cr}}{M_a}\right)\left(\frac{I_e}{I_g}\right) e_g + \left[1-\left(\frac{\lambda_{cr} M_{cr}}{M_a}\right)\right]\left(\frac{I_e}{I_{cr}}\right) e_{cr}$$

$$M_{cr} = \left(f_r + f_{pe}\right) I_g / y_t$$

$$\lambda_{cr} = \left(\frac{2}{3}\right) + \left(\frac{\rho_p}{\rho + \rho_p}\right)\left(\frac{1}{3}\right)$$

Fig. 1: Proposed revision to ACI CODE-318-19, Section 24.2.3.9

Summary of Article Parts

Part 1: Primer for Computing Deflections—Immediate and Time-Dependent
Part 2: New Expression for I_e and Reasons for Change
Part 3: Impact of Changes Made
Part 4: Deflection Example—Continuous Slab
Part 5: Proposed Extension to Prestressed Concrete

Prestressed Concrete Behavior

Figure 2 illustrates the effect of prestressing on the moment-curvature relationship for concrete flexural members. Eccentric prestressing increases the cracking moment and causes an initial upwards deflection (camber) to give a stiffer response at service loads. The axial prestress force also results in a partially cracked section with a nonlinear $E_cI'_{cr}$ response that gradually converges (under increasing load) to the E_cI_{cr} response corresponding to a fully (nonprestressed) cracked section. More importantly, the cracked E_cI_{cr} response is offset from the uncracked E_cI_{tr} response (where the moment M_1 identifies the intersection point of the E_cI_{tr} response and shifted E_cI_{cr} response). The E_cI_{cr} response is shown in Fig. 2 as lying below the cracking moment M_{cr} but can lie above M_{cr} for higher levels of prestressing.[8]

Calculation of deflection is simplified by using the E_cI_{cr} response instead of $E_cI'_{cr}$.[7,9] This avoids the difficulty of locating the neutral axis and then the centroid location, which is not coincident with the neutral axis for a partially cracked section. Other simplifications include approximating the uncracked moment of inertia I_{tr} with the gross moment of inertia I_g and using the effective prestress force P_e in place of the fictitious decompression (prestress) force $P_o = f_{dc}A_{ps}$ described by Nilson.[10] The prestressing force is moved up to the centroid for analysis, resulting in an eccentric prestress moment $P_oe_{cr} \approx P_ee_{cr}$, where e_{cr} is the eccentricity of the prestressing steel relative to the centroid of the cracked section (located at the neutral axis for a fully cracked section).

The decompression stress f_{dc} is defined as the stress in the tendon corresponding to zero stress in the concrete at the level of the prestressed tendons, and A_{ps} is the area of prestressed longitudinal tension reinforcement. The effective prestress force is $P_e = f_{se}A_{ps}$, where f_{se} is the effective stress in the prestressed reinforcement after all losses, including shrinkage and creep. The increased cracking moment associated with prestressing is $M_{cr} = (f_r + f_{pe})\, I_g/y_t$, where f_{pe} is the compressive stress in concrete at the precompressed tensile face resulting from the effective prestress force P_e acting on the deformed section and thus also accounts for losses from creep and shrinkage.

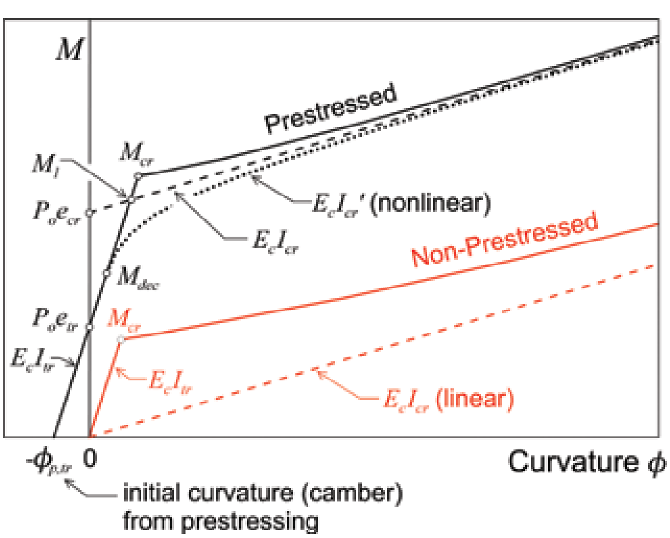

Fig. 2: Comparative plots of moment-curvature relationships for prestressed and reinforced (nonprestressed) flexural members

Model Extension to Prestressed Concrete

Deformation of a cracked prestressed concrete member is modeled by adding a tension stiffening moment $\Delta M_{ts} = \beta_{ts}\,\Delta M_{cr} \le \Delta M_{cr}$ onto the cracked E_cI_{cr} response, as shown in Fig. 3.[7,9] This is similar to the approach used for reinforced (nonprestressed) concrete described in Part 2 of the article series,[2] except the E_cI_{cr} response has been shifted upwards relative to the uncracked E_cI_{tr} response. Model development for prestressed concrete mirrors the steps taken in Part 2 of the article series[2] for reinforced concrete.

The moment M_a for a corresponding curvature ϕ_a is defined as

$$M_a = E_cI_{cr}\left(\phi_a + \phi_{p,cr}\right) + \beta_{ts}\Delta M_{cr} \tag{1a}$$

Rearrangement of terms leads to

$$\phi_a = \frac{M_a}{E_cI_{cr}}\left[1 - \beta_{ts}\left(\frac{\Delta M_{cr}}{M_a}\right)\right] - \phi_{p,cr} \tag{1b}$$

Substituting $\Delta M_{cr} = M_{cr}\left(1 - I_{cr}/I_{tr}\right) - E_cI_{cr}\left(\phi_{p,cr} - \phi_{p,tr}\right)$ into Eq. (1b) gives

$$\phi_a = \frac{M_a}{E_cI_{cr}}\left[1 - \beta_{ts}\left(\frac{M_{cr}}{M_a}\right)\left(1 - \frac{I_{cr}}{I_{tr}}\right)\right] - \left[\beta_{ts}\phi_{p,tr} + \left(1 - \beta_{ts}\right)\phi_{p,cr}\right] \tag{1c}$$

which leads to the curvature $\phi_a = M_a/(E_cI_e) - \phi_{pe}$ for an effective moment of inertia I_e and effective curvature from

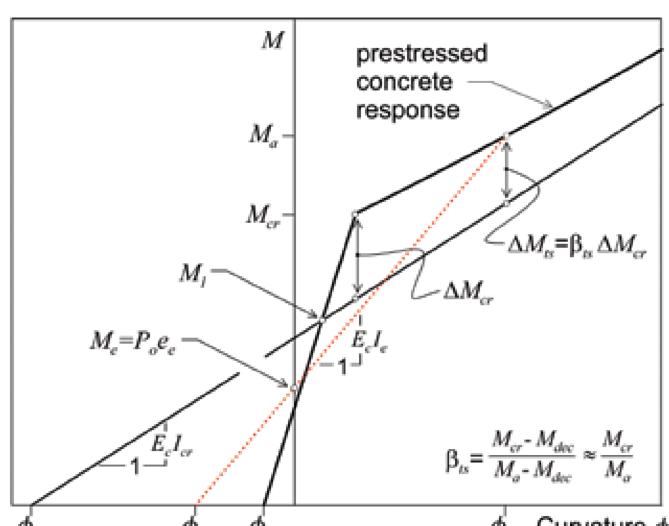

Fig. 3: Model response of prestressed member with tension stiffening

prestressing ϕ_{pe}, defined as

$$I_e = \frac{I_{cr}}{1-\beta_{ts}\left(\frac{M_{cr}}{M_a}\right)\left(1-\frac{I_{cr}}{I_{tr}}\right)} \tag{2a}$$

and

$$\phi_{pe} = \beta_{ts}\phi_{p,tr} + (1-\beta_{ts})\phi_{p,cr} \tag{2b}$$

The curvature from prestressing of an uncracked section, $\phi_{p,tr}$, is given by $\phi_{p,tr} = P_o e_{tr}/(E_c I_{tr})$, and the curvature from prestressing of a fully cracked section, $\phi_{p,cr}$, is given by $\phi_{p,cr} = P_o e_{cr}/(E_c I_{cr})$. ΔM_{ts} decreases with increasing load after cracking using an assumed tension stiffening factor $\beta_{ts} = M_{cr}/M_a$ that is substituted into Eq. (2a) and (2b). Plus, the terms for the uncracked transformed section (I_{tr}, $\phi_{p,tr}$, and e_{tr}) are approximated with the terms for a gross (uncracked) section (I_g, $\phi_{p,g}$, and e_g) to give simplified design expressions for I_e and ϕ_{pe}.

$$I_e = \frac{I_{cr}}{1-\left(\frac{M_{cr}}{M_a}\right)^2\left(1-\frac{I_{cr}}{I_g}\right)} \tag{3a}$$

$$\phi_{pe} = \left(\frac{M_{cr}}{M_a}\right)\phi_{p,g} + \left[1-\left(\frac{M_{cr}}{M_a}\right)\right]\phi_{p,cr} \tag{3b}$$

One final step is taken by setting $P_o e_e = (E_c I_e)\phi_{pe}$ to define an effective eccentricity e_e. Making another simplification by approximating P_o with P_e (essentially estimating the decompression stress f_{dc} with the effective prestress f_{se}), where $\phi_{p,g} = P_e e_g/(E_c I_g)$ and $\phi_{p,cr} = P_e e_{cr}/(E_c I_{cr})$, leads to

$$e_e = \left(\frac{M_{cr}}{M_a}\right)\left(\frac{I_e}{I_g}\right)e_g + \left[1-\left(\frac{M_{cr}}{M_a}\right)\right]\left(\frac{I_e}{I_{cr}}\right)e_{cr} \tag{3c}$$

Curvature is then computed as $\phi_a = (M_a - P_e e_e)/(E_c I_e)$. Figure 4 illustrates the member response calculated when the $E_c I_{cr}$ response lies either below or above the cracking moment.

Shrinkage Restraint from Nonprestressed Reinforcement

The cracking moment $M_{cr} = (f_r + f_{pe})I_g/y_t$ is not reduced for a fully prestressed (FP) member (where the section does not include nonprestressed reinforcement). This is because shrinkage and creep are already taken into account with the effective stress f_{se} in the prestressing steel used to establish the effective prestress force P_e and subsequent compressive stress f_{pe} at the precompressed tensile face (that in turn is used to compute M_{cr}). However, a reduced cracking moment $\lambda_{cr}M_{cr}$ is needed for a prestressed member reinforced with additional nonprestressed reinforcement (defined as partially prestressed [PP] in this article) to account for tensile stresses that develop in the concrete from restraint to shrinkage by the nonprestressed reinforcement.[11] The reduction factor $\lambda_{cr} = \left(\frac{2}{3}\right) + \left(\frac{\rho_p}{\rho+\rho_p}\right)\left(\frac{1}{3}\right)$ varies between 2/3 for a reinforced (nonprestressed) concrete member (identical to ACI CODE-318-19 for nonprestressed concrete) and 1 for an FP member. Substitution of the reduced cracking moment into Eq. (3) then gives

$$I_e = \frac{I_{cr}}{1-\left(\frac{\lambda_{cr}M_{cr}}{M_a}\right)^2\left(1-\frac{I_{cr}}{I_g}\right)} \tag{4a}$$

$$\phi_{pe} = \left(\frac{\lambda_{cr}M_{cr}}{M_a}\right)\phi_{p,g} + \left[1-\left(\frac{\lambda_{cr}M_{cr}}{M_a}\right)\right]\phi_{p,cr} \tag{4b}$$

$$e_e = \left(\frac{\lambda_{cr}M_{cr}}{M_a}\right)\left(\frac{I_e}{I_g}\right)e_g + \left[1-\left(\frac{\lambda_{cr}M_{cr}}{M_a}\right)\right]\left(\frac{I_e}{I_{cr}}\right)e_{cr} \tag{4c}$$

Gross section properties (I_g, $\phi_{p,g}$, e_g) are used for an uncracked member when $M_a \leq \lambda_{cr}M_{cr}$.

Evaluation

Full details on this approach's level of accuracy based on comparison with an extensive database of tests using the results of 180 beams from 23 studies are provided elsewhere.[7] These beams had either rectangular, single tee, or I shapes; were simply supported; had a straight prestressed tendon profile with constant eccentricity; and were subjected to two symmetrically placed point loads.[11] Figure 5 shows a wide scatter of results from these tests as expected, where experimental deflections Δ_{exp} (including camber and member self-weight) are compared with calculated values Δ_{calc} using

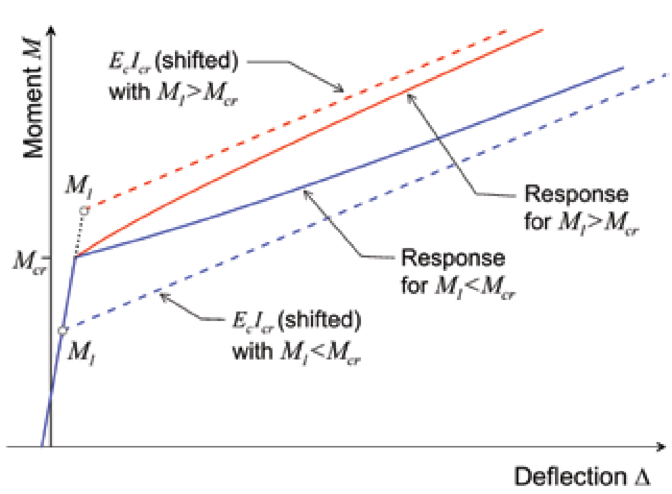

Fig. 4: Calculated prestressed response options

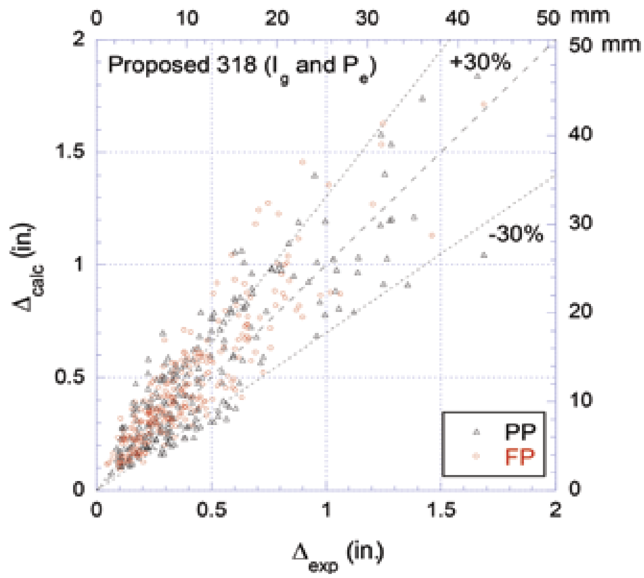

Fig. 5: Calculated versus experimental deflections for fully prestressed (FP) and partially prestressed (PP) beams (using database compiled in Reference 11)

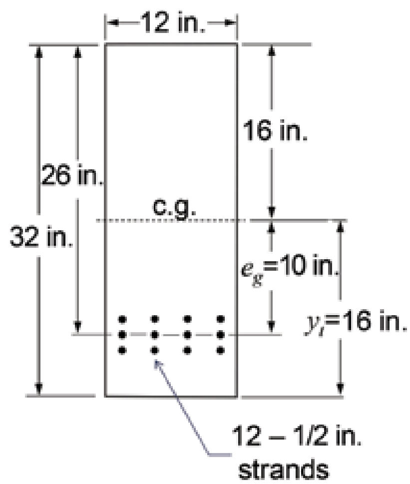

Fig. 6: Prestressed beam example details

the procedure described in the deflection example. Deflection is overestimated by a moderate amount on average, with a mean deflection prediction ratio ($\Delta_{calc}/\Delta_{exp}$) equal to 1.24 when deflection values are computed directly (based on net curvature calculations as shown in the example). Integrating curvature (based on I_e and e_e calculated at each section along the member span) decreases the mean $\Delta_{calc}/\Delta_{exp}$ ratio to a value of 1.06. Using the decompression prestress force P_o and properties of the uncracked transformed section to determine M_{cr}, I_e, and e_e further improves prediction of deflection.[7]

Prestressed Deflection Example

Example 5.2.2.5 taken from the 2010 PCI Design Handbook[12] and based on Example 1 from Mast's PCI paper[13] is used to demonstrate the proposed approach for computing immediate deflection of a simply supported prestressed beam cracked under service load. The prestressed beam is rectangular, as shown in Fig. 6, and prestressed with twelve 1/2 in. diameter 270 K strands located at an effective depth d_p = 26 in. The span ℓ = 40 ft, f_c' = 6000 psi, and $E_c = 57{,}000\sqrt{f_c'} = 4415$ ksi to give $n_p = E_p/E_c = 6.46$ (assuming E_p = 28,500 ksi).

Loads and midspan moments are as follows:

Self-weight = 150 lb/ft^3 × (12/12)ft × (32/12)ft ÷ 1000 = 0.40 kip/ft
Superimposed dead load = 1.0 kip/ft
Total dead load = 1.4 kip/ft
Live load = 1.25 kip/ft
$M_D = 1.4 \times 40^2/8$ = 280 kip-ft = 3360 kip-in.
$M_L = 1.25 \times 40^2/8$ = 250 kip-ft = 3000 kip-in.
$M_a = M_D + M_L$ = 530 kip-ft = 6360 kip-in.

Prestress force details are as follows:

$A_{ps} = 12 \times 0.153 = 1.836$ in.^{2}
$\rho_p = A_{ps}/(bd_p) = 1.836/(12 \times 26) = 0.0059$
(plus $\rho = 0$ because there is no nonprestressed reinforcement)
f_{pu} = 270 ksi
Initial prestress level = $0.75f_{pu}$ and estimated loss of 20% gives f_{se} = (1 – 0.20)(0.75)(270) = 162.0 ksi
$P_e = 1.836 \times 162.0 = 297.4$ kip

Section properties are as follows:

A_g = 384 in.^{2} and I_g = 32,768 in.^{4}
y_t = 16 in. and e_g = 26 – 16 = 10 in. (see Fig. 6)
$f_{pe} = P_e/A_g + (P_e \times e_g)\, y_t/I_g$ = 297.4/384 + (297.4 × 10) × 16/32,768 = 2.227 ksi
$f_r = 7.5\sqrt{f_c'} = 7.5\sqrt{6000} = 581$ psi
$M_{cr} = (f_r + f_{pe})\, I_g/y_t$ = (0.581 + 2.227)32,768/16 = 5750 kip-in.
λ_{cr} = (2/3) + [0.0059/(0 + 0.0059)](1/3) = 1.0 and $\lambda_{cr}M_{cr}$ = 5750 kip-in.
$n_p\rho_p = 6.46 \times 0.0059 = 0.038$

$$k_{cr} = \sqrt{\left(n_p\rho_p\right)^2 + 2\left(n_p\rho_p\right)} - \left(n_p\rho_p\right) = \sqrt{(0.038)^2 + 2\times 0.038} - 0.038 = 0.240$$

$c_{cr} = k_{cr} \times d_p = 0.240 \times 26 = 6.24$ in. and e_{cr} = 26 – 6.24 = 19.76 in.
(the centroid is located at the neutral axis because the section is fully cracked)
$I_{cr} = b(c_{cr})^3/3 + n_pA_{ps}\,(d_p - c_{cr})^2$ = $12 \times (6.24)^3/3 + 6.46 \times 1.836 \times (26 - 6.24)^2$ = 5603 in.^{4}
Using the PCI[12] approximation for $I_{cr} = n_pA_{ps}d_p^{\,2}\left(1 - 1.6\sqrt{n_p\rho_p}\right)$ gives

$$I_{cr} = 6.46 \times 1.836 \times 26^2 \times \left(1 - 1.6\sqrt{0.038}\right) = 5517 \text{ in.}^4$$

This approximation works reasonably well for ρ_p up to about 0.5% but can underestimate I_{cr} significantly at higher reinforcement ratios.[11]

Deflection calculations are as follows:

The section is cracked under the full dead plus live service

load with
$M_a = 6360 > \lambda_{cr}M_{cr} = 5750$ kip-in.
$\lambda_{cr}M_{cr}/M_a = 0.904$

$$I_e = \frac{5603}{1-(0.904)^2(1-5603/32,768)} = 17,373 \text{ in.}^4$$

$$e_e = 0.904 \times \left(\frac{17,373}{32,768}\right) \times 10 + (1-0.904) \times \left(\frac{17,373}{5603}\right) \times 19.76 = 10.67$$

Curvature ϕ_a at M_a is calculated as
$\phi_a = M_a/(E_cI_e) - P_e \times e_e/(E_cI_e) = (M_a - P_e \times e_e)/(E_cI_e) =$
$(6360 - 297.4 \times 10.67)/(4415 \times 17,373) = 41.55 \times 10^{-6}$ 1/in.
Referring to Fig. 7, the net curvature $\phi_{net} = \phi_a + \phi_{p,g} = \phi_D + \phi_L$
with $\phi_{p,g} = P_e \times e_g/(E_cI_g) = 297.4 \times 10/(4415 \times 32,768) =$
20.56×10^{-6} 1/in.
and $\phi_D = M_D/(E_cI_g) = 3360/(4415 \times 32,768) =$
23.22×10^{-6} 1/in.
$\therefore \phi_{net} = (41.55 + 20.56) \times 10^{-6} = 62.11 \times 10^{-6}$ 1/in.
and $\phi_L = \phi_{net} - \phi_D = (62.11 - 23.22) \times 10^{-6} = 38.89 \times 10^{-6}$ 1/in.
Net deflection $\Delta_{net} = K_M\phi_{net}\ell^2$ (with $K_M = 5/48$ for an assumed parabolic distribution of curvature as shown in Fig. 7).
$\Delta_{net} = (5/48) \times 62.11 \times (40 \times 12)^2 \times 10^{-6} = 1.491$ in.
$\Delta_a = \Delta_{net} - \Delta_{p,g} = 1.491 - 0.592 = 0.899$ in.
with $\Delta_{p,g} = K_p\phi_{p,g}\ell^2 = (1/8) \times 20.56 \times (40 \times 12)^2 \times 10^{-6} =$
0.592 in. $K_p = 1/8$ for a simply supported member with straight tendons having constant eccentricity.
Live load deflection $\Delta_{i,L} = \Delta_{net} - \Delta_{i,D}$ with $\Delta_{i,D} = (5/48)\phi_D\ell^2$.
$\Delta_{i,D} = (5/48) \times (23.22 \times 10^{-6}) \times (40 \times 12)^2 = 0.557$ in.
and $\Delta_{i,L} = 1.491 - 0.557 = 0.934$ in. Alternatively,

$$\Delta_{i,L} = K_M\phi_L\ell^2 = \left(\frac{5}{48}\right) \times (38.89 \times 10^{-6}) \times (40 \times 12)^2 = 0.933 \approx 0.934 \text{ in.}$$

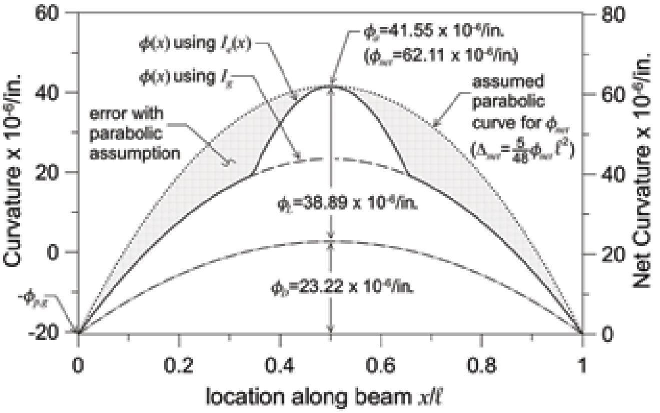

Fig. 7: Curvature distribution for beam example

The estimated value of $\Delta_{i,L} = 0.934$ in. overestimates live load deflection by 36% compared to a value of 0.688 in. obtained by integrating curvature, while the value for $\Delta_a = 0.899$ in. overestimates deflection by about the same amount compared to the value of 0.653 in. when curvature is integrated. The shaded area in Fig. 7 represents the error when computing deflection with the net curvature approximated by a parabolic curve (assuming the load is uniformly distributed).

Approximating the net curvature with a linear distribution response (triangular in shape with $\phi_{net} = 62.11 \times 10^{-6}$ 1/in. at the apex located at midspan) gives values of $\Delta_{i,L} = 0.635$ in. and $\Delta_a = 0.600$ in., which underestimate deflection by about 8% in each case compared to integrating curvature.

Comparison can also be made with the more exact approach based on P_o and the uncracked transformed section properties (I_{tr}, $\phi_{p,tr}$, and e_{tr}) used to determine M_{cr}, I_e, and e_e.

The decompression stress $f_{dc} = f_{se} + n_p\left(\frac{P_e}{A_g} + \frac{P_e(e_g)^2}{I_g}\right) = 172.9$ ksi and the decompression prestress force $P_o = f_{dc} \times A_{ps} = 317.4$ kip to give a higher cracking moment $M_{cr} = 6065$ kip-in. (acting on the uncracked transformed section). The higher cracking moment decreases the computed deflection from live load considerably (from 0.934 in. to 0.690 in. using the parabolic approximation for net curvature) because of the closer proximity of the service load moment $M_a = 6360$ kip-in. to the increased value of the cracking moment (increasing from 5750 to 6065 kip-in.). Computed values of live load deflection range between 48 and 70% of the ACI CODE-318 limit of $\ell/360 = 1.33$ in. for this example, depending of course on the procedure used to calculate deflection.

Fully prestressed (FP): prestressed member with prestressed reinforcement only

Partially prestressed (PP): prestressed member with prestressed and nonprestressed reinforcement

Summary

The ACI CODE-318-19 approach for calculating immediate deflection of reinforced (nonprestressed) concrete is broadened to include prestressed concrete loaded above the cracking moment (Class T and Class C prestressed members). A rational mechanical model is used as the basis for adding a tension stiffening component (in this case moment) onto the cracked E_cI_{cr} response that is shifted upwards relative to the

Deflection computed directly based on net curvature ϕ_{net}:

$$\phi_a = \frac{M_a - P_e e_e}{E_c I_e}$$

$$\phi_{p,g} = \frac{P_e e_g}{E_c I_g}$$

$$\phi_{net} = \phi_a + \phi_{p,g}$$

$$\phi_{net} = \phi_D + \phi_L$$

$$\phi_D = \frac{M_D}{E_c I_g}$$

$$\phi_L = \phi_{net} - \phi_D$$

$$\Delta_{net} = K_M \phi_{net} \ell^2$$

$$\Delta_{p,g} = K_p \phi_{p,g} \ell^2$$

$$\Delta_a = \Delta_{net} - \Delta_{p,g}$$

$$\Delta_{i,D} = K_M \phi_D \ell^2$$

$$\Delta_{i,L} = \Delta_{net} - \Delta_{i,D}$$

or

$$\Delta_{i,L} = K_M \phi_L \ell^2$$

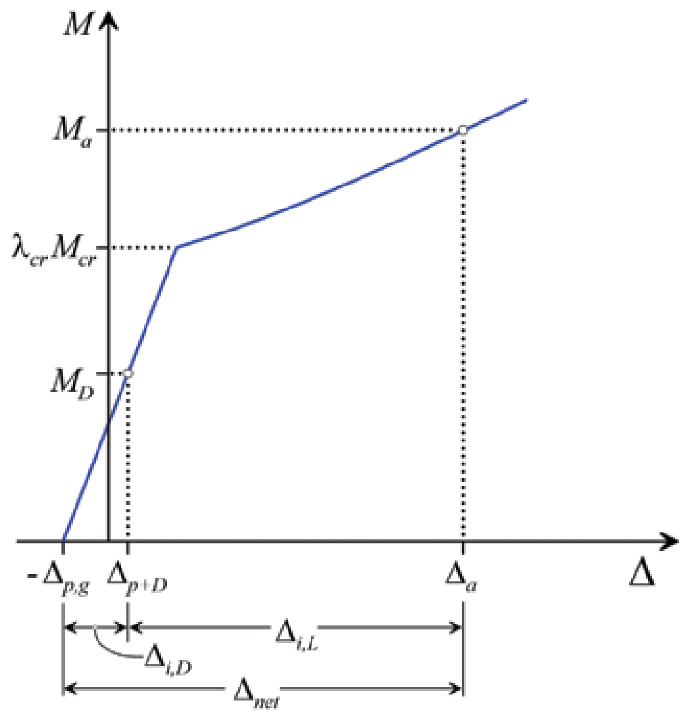

$K_M = \frac{5}{48}$ for simply supported beam with uniformly distributed load

$K_p = \frac{1}{8}$ for simply supported beam using straight tendon with constant eccentricity uncracked E_cI_g response because of the eccentric prestressing force. The proposed approach summarized in Fig. 1 for prestressed concrete includes an effective moment of inertia I_e and effective eccentricity e_e of the prestressing force when the member is cracked. I_g and e_g are used for an uncracked member. The cracking moment is reduced with a reduction factor λ_{cr} to account for tensile stresses that develop in the concrete from restraint to shrinkage by the nonprestressed reinforcement when present. Procedures are presented for computing deflection directly based on net curvature (using an assumed uniform value of I_e and e_e at the critical section) and compared with deflection computed by integrating curvature (using I_e and e_e calculated at each section along the member span). The PCI bilinear load-deflection response is also considered in the bonus example.

Acknowledgments

Insightful comments and suggestions by Rex Donahey during the writing of this article series (Parts 1 to 5) are much appreciated.

References

1. Bischoff, P.H., "Computing Deflections Using ACI CODE-318-19 and Beyond, Part 1," *Concrete International*, V. 47, No. 2, Feb. 2025, pp. 47-50.

2. Bischoff, P.H., "Computing Deflections Using ACI CODE-318-19 and Beyond, Part 2," *Concrete International*, V. 47, No. 3, Mar. 2025, pp. 51-54.

3. Bischoff, P.H., "Computing Deflections Using ACI CODE-318-19 and Beyond, Part 3," *Concrete International*, V. 47, No. 4, Apr. 2025, pp. 47-50.

4. Bischoff, P.H., "Computing Deflections Using ACI CODE-318-19 and Beyond, Part 4," *Concrete International*, V. 47, No. 5, May 2025, pp. 62-65.

5. ACI Committee 318, "Building Code Requirements for Structural Concrete (ACI 318-19) and Commentary (ACI 318R-19)," American Concrete Institute, Farmington Hills, MI, 2019, 624 pp.

6. Branson, D.E., *Deformation of Concrete Structures*, McGraw-Hill, New York, NY, 1977, 546 pp.

7. Bischoff, P.H.; Nasreddine, W.; and Nassif, H., "Proposed ACI 318 Equations for Immediate Deflection of Prestressed Concrete Members," *ACI Structural Journal*, V. 122, No. 6, Nov. 2025, pp. 127-139.

8. Bischoff, P.H.; Naito, C.J.; and Ingaglio, J.P., "Immediate Deflection of Partially Prestressed Concrete Flexural Members," *ACI Structural Journal*, V. 115, No. 6, Nov. 2018, pp. 1683-1693.

9. Bischoff, P.H., "Deformation Model for Reinforced and Cracked Prestressed Concrete," *ACI Structural Journal*, V. 119, No. 1, Jan. 2022, pp. 243-254.

10. Nilson, A.H., "Flexural Stresses After Cracking in Partially Prestressed Beams," *PCI Journal*, V. 21, No. 4, July-Aug. 1976, pp. 72-81.

11. Nasreddine, W.; Obeidah, A.; Bischoff, P.H.; and Nassif, H., "Assessment of Deflection Prediction Models for Cracked Prestressed Concrete Beams," *ACI Structural Journal*, V. 120, No. 6, Nov. 2023, pp. 167-179.

12. PCI, *PCI Design Handbook: Precast and Prestressed Concrete*, seventh edition, Precast/Prestressed Concrete Institute, Chicago, IL, 2010, 804 pp.

13. Mast, R.F., "Analysis of Cracked Prestressed Concrete Sections: A Practical Approach," *PCI Journal*, V. 43, No. 4, July-Aug. 1998, pp. 80-91.

Received and reviewed under Institute publication policies.

Peter H. Bischoff, FACI, is Professor Emeritus in Civil Engineering at the University of New Brunswick, Fredericton, NB, Canada. He is a member of ACI Committees 224, Cracking; 435, Deflection of Concrete Building Structures; 440, Fiber-Reinforced Polymer Reinforcement; and 440C, FRP Reinforced Concrete Building Code. He received the ACI Design Award in 2014, ASCE T.Y. Lin Award in 2020 for an *ACI Structural Journal* paper related to deflection of prestressed concrete, and the ACI Symposium Volumes Award in 2025. His research interests include the serviceability behavior of concrete structures.

ACI member **Wassim Nasreddine** is a Research Associate at Rutgers, The State University of New Jersey, New Brunswick, NJ, USA. He is a member of ACI Committees 435, Deflection of Concrete Building Structures, and 440, Fiber-Reinforced Polymer Reinforcement. He received the ACI Symposium Volumes Award in 2025. His research interests include prestressed concrete member behavior, innovative concrete materials, and strengthening and retrofitting of concrete structures.

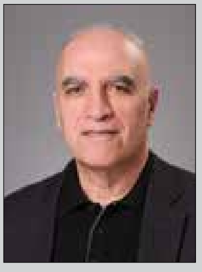

Hani Nassif, FACI, is a Professor of structural engineering at Rutgers, The State University of New Jersey. He is a past member of the ACI Technical Activities Committee (TAC); Chair of ACI Committee 549, Thin Reinforced Cementitious Products and Ferrocement; Vice Chair of ACI Subcommittee 440-I, FRP-Prestressed Concrete; and is a member of ACI Committees 209, Creep and Shrinkage in Concrete; 343, Concrete Bridge Design; 348, Structural Reliability and Safety; 435, Deflection of Concrete Building Structures; 440, Fiber-Reinforced Polymer Reinforcement; and 444, Structural Health Monitoring. He received the Arthur J. Boase Award and ACI Symposium Volumes Award, both in 2025. His research focuses on structural concrete and the use of advanced cementitious and composite materials.

Appendix: Bonus Deflection Example

This bonus example is taken from Example 5.8.3.1 (based on details from Example 5.2.2.3) of the PCI Design Handbook,[12] where immediate deflection from live load is calculated for a Class T double tee (8DT24)—that is prestressed with the strands harped at midspan (single-point depressed strands). The beam is simply supported with a span ℓ = 70 ft.

Two alternative procedures are presented for direct calculation of immediate deflection based on either a parabolic or trapezoidal approximation for the distribution of net curvature along the member span. Comparison is made with deflection computed using integration of curvature based on the effective eccentricity e_e and effective moment of inertia I_e corresponding to each section along the member span (with e_g and I_g used in the uncracked regions). Plus, results are presented for deflection calculation using the PCI bilinear load-deflection response. Calculation in some parts is carried out with more precision than needed (in terms of significant figures) to facilitate comparison of results.

Beam gross section properties

The cross section of the 24 in. deep PCI double tee shown in Fig. A1 has the following section properties for the gross (uncracked) section.

A_g = 401 in.^{2} and I_g = 20,985 in.^{4}

y_{top} = 6.85 in. and y_{bot} = 17.15 in.

w_{sw} = 150 lb/ft^3 × 401 in.^{2} ÷ 12 ÷ 12 = 418 lb/ft (distributed line load for self-weight)

Prestressing details

The beam is prestressed with twelve 1/2 in. diameter, 270 ksi, low-relaxation strands. This gives A_{ps} = 12 × 0.153 = 1.836 in.^{2}

The strands have a single harping point at midspan, giving a straight tendon with variable eccentricity. Eccentricities are as follows:

$e_{g,end}$ = 5.48 in. (eccentricity of prestressing force at end of span)

$e_{g,c}$ = 13.90 in. (eccentricity of prestressing force at midspan)

θ = (13.90 – 5.48)/(70 × 12/2) = 20.05 × 10^{-3} rads (angle of inclination for centroid of prestressing strands)

$e_g(x) = e_{g,end} + \theta x$ (eccentricity at distance x from end of span for $x \leq \ell/2$)

$e_g(0.4\ell)$ = 5.48 + 20.05 × 10^{-3} × (0.4 × 70 × 12) = 12.216 in. (eccentricity at 0.4ℓ)

The effective depth d_p of the prestressing steel and moment of inertia of the cracked section I_{cr} vary along the member span as the eccentricity changes.

d_p = 6.85 + 13.90 = 20.75 in. at 0.5ℓ

d_p = 6.85 + 12.216 = 19.066 in. at 0.4ℓ

Initial prestress level = 0.75f_{pu} and estimated loss equals 20%

f_{se} = (1 – 0.20)(0.75)(270) = 162.0 ksi

$P_e = A_{ps} \times f_{se}$ = 1.836 × 162.0 = 297.4 kip and is assumed constant along the beam span.

Concrete design properties

The concrete has a specified compressive strength f_c' = 5000 psi, giving $f_r = 7.5\sqrt{f_c'} = 7.5\sqrt{5000} = 530$ psi and $E_c = 33w_c^{1.5}\sqrt{f_c'} = 33(145)^{1.5}\sqrt{5000}/1000 = 4074$ ksi. Using w_c = 145 lb/ft^3 for normalweight concrete gives $E_c \approx 57,000\sqrt{f_c'}$. The modular ratio $n_p = E_p/E_c$ = 28,500/4074 = 7.0 (assuming E_p = 28,500 ksi).

Member loads

Member self-weight w_{sw} = 418 lb/ft (from beam gross section properties)

Superimposed dead load w_{sd} = 10 lb/ft^2 × 8 ft = 80 lb/ft

Total dead load w_D = 418 + 80 = 498 lb/ft

Live load w_L = 35 lb/ft^2 × 8 ft = 280 lb/ft

Service load moments

The critical moment occurs at midspan (0.5ℓ) for beams with straight strands of constant eccentricity and is assumed to occur at 0.4ℓ for beams when the strands are depressed at midspan, as with this example.[12] For the prestressed beam in this example, the actual critical section occurs at 0.39ℓ for the maximum value of total bottom stress f_b in the concrete at the precompressed tension face, and at 0.384ℓ for the maximum value of M/M_{cr} (details are provided further on in Aside 1).

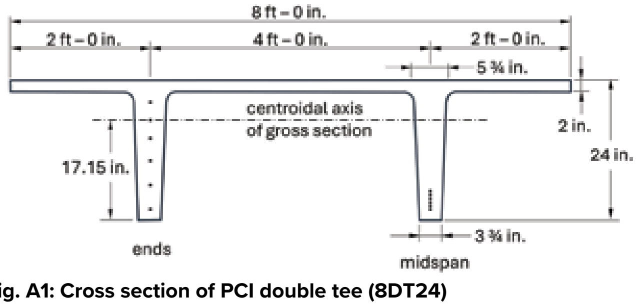

Fig. A1: Cross section of PCI double tee (8DT24)

Figure A2 plots the distribution of f_b/f_r and M/M_{cr} along the member span. Negative values of the bottom stress for f_b (indicating compression) that occur in the region near the end support are not plotted in this figure.

Service load moments at midspan ($\ell/2$) are as follows:

$M_D(\ell/2) = w_D\ell^2/8 = 498 \div 12 \div 1000 \times (70 \times 12)^2/8 =$ 3660.3 kip-in.

$M_L(\ell/2) = w_L\ell^2/8 = 280 \div 12 \div 1000 \times (70 \times 12)^2/8 =$ 2058.0 kip-in.

$M_a = M_{D+L}(\ell/2) = M_D(\ell/2) + M_L(\ell/2) = 5718.3$ kip-in.

Service load moments at the critical section (0.4ℓ) are equal to 0.96 times the moment at midspan based on a parabolic distribution of moment from the uniformly distributed loads.

$M_D(0.4\ell) = 0.96M_D(0.5\ell) = 0.96 \times 3660.3 = 3513.9$ kip-in.

$M_L(0.4\ell) = 0.96M_L(0.5\ell) = 0.96 \times 2058.0 = 1975.7$ kip-in.

$M(0.4\ell) = M_{D+L}(0.4\ell) = 0.96M_a = 0.96 \times 5718.3 =$ 5489.6 kip-in.

where M_a is the total dead plus live load moment at midspan (0.5ℓ).

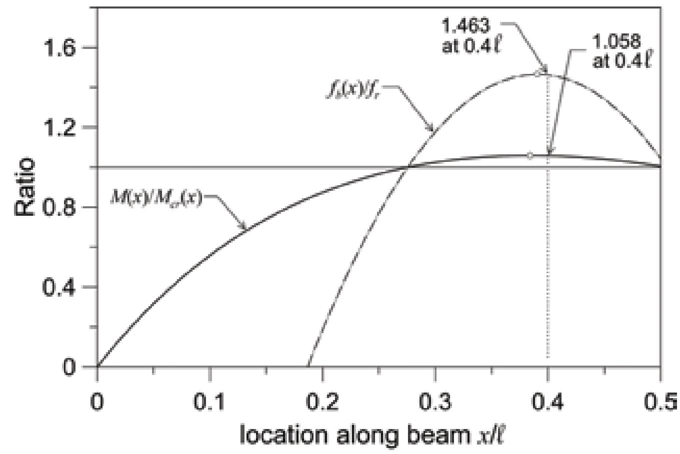

Fig. A2: Distribution of $f_b(x)/f_r$ and $M(x)/M_{cr}(x)$ along the beam span

Critical section properties (at 0.4ℓ)

When deflection is computed directly, a constant value of member stiffness EI and eccentricity e of the prestressing force is assumed based on the effective moment of inertia I_e and effective eccentricity e_e at the critical section located at 0.4ℓ. The section is cracked at 0.4ℓ, but barely cracked at midspan (0.5ℓ) as observed from Fig. A2.

The stress f_{pe} at the bottom precompressed face from prestress only is used to calculate the cracking moment at 0.4ℓ.

$$f_{pe}(0.4\ell) = \frac{P_e}{A_g} + \frac{P_e e_g(0.4\ell)y_{bot}}{I_g} = \left(\frac{297.4}{401} + \frac{297.4(12.216)(17.15)}{20,985}\right)\times 1000 = 3710.75 \text{ psi (C)}$$

$$M_{cr}(0.4\ell) = \left[f_r + f_{pe}(0.4\ell)\right]\frac{I_g}{y_{bot}} = \frac{(530+3710.75)\left(\frac{20,985}{17.15}\right)}{1000} = 5189.0 \text{ kip-in.}$$

$$\frac{M_{cr}(0.4\ell)}{M(0.4\ell)} = \frac{5189.0}{5489.6} = 0.9452$$

Hence, $\lambda_{cr}M_{cr}/M = 0.9452$ at the critical location (0.4ℓ). Recall that $\lambda_{cr} = 1$ for a prestressed section with no nonprestressed reinforcement.

The neutral axis of the fully cracked section extends into the web at 0.4ℓ, giving $I_{cr} = 3993$ in.^{4} with a value of the neutral axis depth $c_{cr} = 2.13$ in. and eccentricity $e_{cr} = d_p - c_{cr} = 19.066 - 2.13 = 16.936$ in. Compare this with the PCI approximation for $I_{cr} = n_p A_{ps} d_p^2\left(1 - 1.6\sqrt{n_p\rho_p}\right) = 4046$ in.^{4} (a little more than a 1% difference in this case) given $n_p = 7.0$, $A_{ps} = 1.836$ in.^{2}, $d_p = 19.066$ in. at 0.4ℓ, and $\rho_p = 1.836/(96 \times 19.066) = 0.0010$ at 0.4ℓ.

Effective section properties at the critical section (0.4ℓ) are as follows:

$$I_e(0.4\ell) = \frac{I_{cr}(0.4\ell)}{1 - \left(\frac{\lambda_{cr}M_{cr}(0.4\ell)}{M(0.4\ell)}\right)^2\left(1 - \frac{I_{cr}(0.4\ell)}{I_g}\right)} = \frac{3993}{1 - (0.9452)^2\left(1 - \frac{3993}{20,985}\right)} = 14,436 \text{ in.}^4$$

$$e_e(0.4\ell) = \left(\frac{\lambda_{cr}M_{cr}(0.4\ell)}{M(0.4\ell)}\right)\left(\frac{I_e(0.4\ell)}{I_g}\right)e_g(0.4\ell) + \left[1 - \left(\frac{\lambda_{cr}M_{cr}(0.4\ell)}{M(0.4\ell)}\right)\right]\left(\frac{I_e(0.4\ell)}{I_{cr}(0.4\ell)}\right)e_{cr}(0.4\ell) =$$

$$(0.9452)\left(\frac{14,436}{20,985}\right)12.216 + \left[1 - (0.9452)\right]\left(\frac{14,436}{3993}\right)16.936 = 11.30 \text{ in.}$$

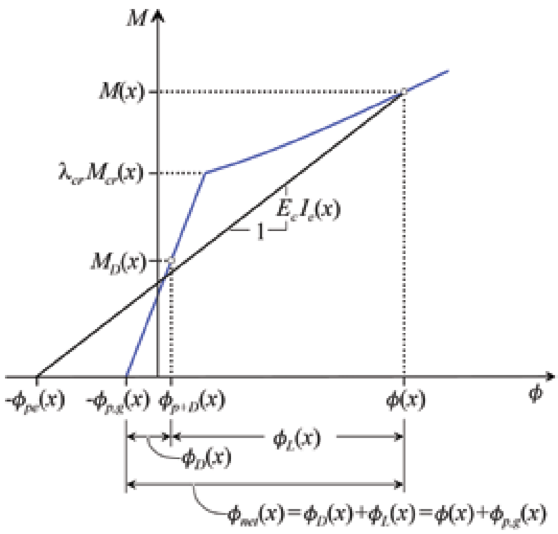

$$I_e(x)=\frac{I_{cr}(x)}{1-\left(\frac{\lambda_{cr}M_{cr}(x)}{M(x)}\right)^2\left(1-\frac{I_{cr}(x)}{I_g}\right)}$$

$$e_e(x)=\left(\frac{\lambda_{cr}M_{cr}(x)}{M(x)}\right)\left(\frac{I_e(x)}{I_g}\right)e_g(x)+\left[1-\left(\frac{\lambda_{cr}M_{cr}(x)}{M(x)}\right)\right]\left(\frac{I_e(x)}{I_{cr}(x)}\right)e_{cr}(x)$$

$$\phi_{pe}(x)=\frac{P_e e_e(x)}{E_c I_e(x)}\ \text{ and }\ \phi_{p,g}(x)=\frac{P_e e_g(x)}{E_c I_g}$$

$$\phi(x)=\frac{M(x)}{E_c I_e(x)}-\phi_{pe}(x)=\frac{M(x)-P_e e_e(x)}{E_c I_e(x)}$$

$$\phi_{p+D}(x)=\frac{M_D(x)}{E_c I_g}-\phi_{p,g}(x)$$

$$\phi_D(x)=\frac{M_D(x)}{E_c I_g}$$

$$\phi_{net}(x)=\phi(x)+\phi_{p,g}(x)=\phi_D(x)+\phi_L(x)$$

$$\phi_L(x)=\phi_{net}(x)-\phi_D(x)=\phi(x)+\phi_{p,g}(x)-\frac{M_D(x)}{E_c I_g}$$

Fig. A3: Moment-curvature response of prestressed beam with relevant equations

Curvatures at the critical section (0.4ℓ)

Corresponding curvatures at the critical section (0.4ℓ) are computed using guidance from Fig. A3 that summarizes the relevant equations for curvature needed to calculate deflection. Values for the section properties and curvatures are summarized in Table A1 for convenience.

$$\phi(0.4\ell)=\frac{M(0.4\ell)-P_e e_e(0.4\ell)}{E_c I_e(0.4\ell)}=\frac{5489.6-297.4\times 11.30}{4074\times 14{,}436}=36.20\times 10^{-6}\ \text{1/in.}$$

$$\phi_{p,g}(0.4\ell)=\frac{P_e e_g(0.4\ell)}{E_c I_g}=\frac{297.4\times 12.216}{4074\times 20{,}985}=42.495\times 10^{-6}\ \text{1/in.}$$

$$\phi_{net}(0.4\ell)=\phi(0.4\ell)+\phi_{p,g}(0.4\ell)=(36.20+42.495)\times 10^{-6}=78.695\times 10^{-6}\ \text{1/in.}$$

$$\phi_D(0.4\ell)=\frac{M_D(0.4\ell)}{E_c I_g}=\frac{3513.9}{4074\times 20{,}985}=41.10\times 10^{-6}\ \text{1/in.}$$

$$\phi_L(0.4\ell)=\phi_{net}(0.4\ell)-\phi_D(0.4\ell)=(78.695-41.10)\times 10^{-6}=37.595\times 10^{-6}\ \text{1/in.}$$

Curvature plots

Plots of the distribution for curvature are shown in Fig. A4 for the prestressing force $\phi_{p,g}(x)$, the dead load plus prestressing force $\phi_{p+D}(x)$, the total (dead and live) load plus prestressing force $\phi(x)$, and for $\phi(x)$ assuming a parabolic distribution of the net curvature $\phi_{net}(x)$ taken from Fig. A5. Notice the curious kink that occurs in the curves near midspan for $\phi_{p+D}(x)$ and $\phi(x)$ as $\phi_{p,g}$ increases towards midspan of the beam. Loss of prestress in the bond transfer length at the beam ends is neglected.

Plots of the curvature from dead load alone $\phi_D(x)$, the net curvature for dead plus live load, $\phi_{net}(x) = \phi_D(x) + \phi_L(x)$, and an

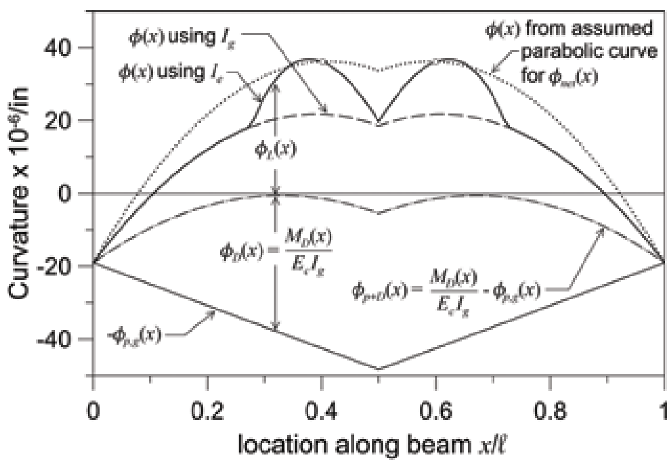

Fig. A4: Curvature distribution for beam example

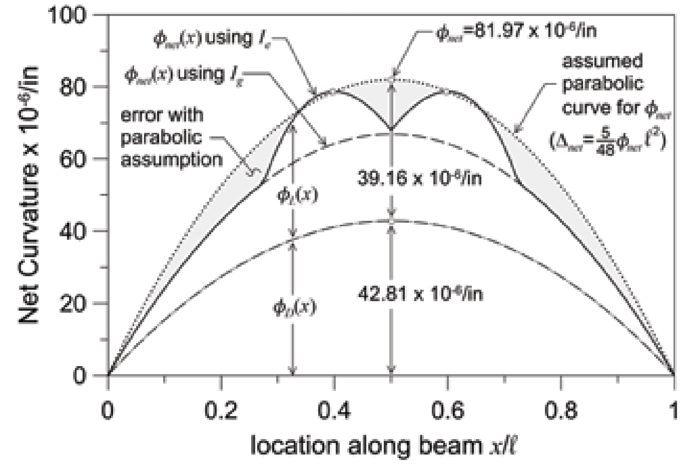

Fig. A5: Net curvature distribution for beam example (approximated with parabolic curve)

assumed parabolic distribution for the net curvature $\phi_{net}(x)$ are shown in Fig. A5. Once again, the increase in $\phi_{p,g}$ toward midspan causes a kink in the net curvature $\phi_{net}(x)$ near midspan (as the effective moment of inertia increases near midspan because of a localized increase in $\lambda_{cr}M_{cr}(x)/M(x)$ as observed from the values in Table A1).

Parabolic approximation for net curvature

Assuming a parabolic curve for the net curvature ϕ_{net} running through the value at 0.4ℓ and having a maximum value at midspan (0.5ℓ) as shown in Fig. A5 gives

$$\phi_{net}\left(0.5\ell\right) \approx \phi_{net}\left(0.4\ell\right)/0.96 = \left(78.695/0.96\right)\times 10^{-6} = 81.97\times 10^{-6} \text{ 1/in.}$$

In a similar fashion, a parabolic curve fitted to the curvature value from live load at 0.4ℓ gives

$$\phi_L\left(0.5\ell\right) \approx \phi_L\left(0.4\ell\right)/0.96 = 37.595\times 10^{-6}/0.96 = 39.16\times 10^{-6} \text{ 1/in.}$$

Deflections based on net curvature using parabolic approximation

Knowing that $K_M = 5/48$ when the distribution of curvature is parabolic, gives

$$\Delta_{i,L} = K_M \phi_L\left(0.5\ell\right)\ell^2 = \frac{5}{48}\times 39.16\times 10^{-6}\times\left(70\times 12\right)^2 = 2.88 \text{ in.}$$

and is about 20% greater than the value of $\Delta_{i,L} = 2.39$ in. when curvature is integrated. Integration takes account of the uncracked regions of the beam (using $e_g(x)$ and I_g) as well as for changes in $e_e(x)$ and $I_e(x)$ in the cracked regions. Figures A2 and A4 indicate the beam is cracked near the midspan region for $0.277 < x/\ell < 0.723$. Alternatively,

$$\Delta_{net} = \frac{5}{48}\phi_{net}\left(0.5\ell\right)\ell^2 = \frac{5}{48}\times 81.97\times 10^{-6}\times\left(70\times 12\right)^2 = 6.025 \text{ in.}$$

$$\Delta_{i,D} = \frac{5}{48}\left[\frac{M_D\left(0.5\ell\right)}{E_c I_g}\right]\ell^2 = \frac{5}{48}\left[\frac{3660.3}{4074\times 20{,}985}\right]\left(70\times 12\right)^2 = 3.15 \text{ in.}$$

$$\Delta_{i,L} = \Delta_{net} - \Delta_{i,D} = 6.025 - 3.15 = 2.875 \approx 2.88 \text{ in. as before.}$$

For the total deflection (that includes the camber from prestress)

$$\Delta_a = \Delta_{net} - \Delta_{p,g} = 6.025 - 3.40 = 2.625 \text{ in.}$$

where

$$\Delta_{p,g} = \left[2 + \frac{e_{g,end}}{e_{g,c}}\right] \times \frac{P_e e_{g,c} \ell^2}{24 E_c I_g} = \left[2 + \frac{5.48}{13.90}\right] \times \frac{297.4 \times 13.90 \times (70 \times 12)^2}{24 \times 4074 \times 20,985} = 3.40 \text{ in.}$$

The PCI Design Handbook[12] provides camber equations needed to compute $\Delta_{p,g}$ for different prestressing strand profiles.

The estimated value of 2.625 in. for Δ_a is 23% greater that the value of 2.14 in. obtained by integrating curvature. These calculations are idealized in part, as the deformations due to prestress (aside from using P_e) and dead load do not account for the effects of creep from sustained loading.

Table A1:
Summary of section properties and curvature values

	Ends*	0.4ℓ	0.5ℓ
A_g, in.^{2}	401	401	401
I_g, in.^{4}	20,985	20,985	20,985
y_{bot}, in.	17.15	17.15	17.15
$e_g(x)$, in.	5.48	12.216	13.90
$d_p(x)$, in.	12.33	19.066	20.75
$\rho_p(x)$	0.00155	0.00100	0.00092
$M_D(x)$, kip-in.	0	3513.9	3660.3
$M_L(x)$, kip-in.	0	1975.7	2058.0
$M(x)$, kip-in.	0	5489.6	5718.3
$f_b(x)$, psi	2073.6 (C)	775.6 (T)†	553.2 (T)
$f_b(x)/f_r$	−3.912	1.463	1.044
$f_{pe}(x)$, psi	2073.6 (C)	3710.75 (C)	4120.0 (C)
$M_{cr}(x)$, kip-in.	3185.8	5189.0	5689.9
λ_{cr}	1.0	1.0	1.0
$\lambda_{cr}M_{cr}(x)/M(x)$	---	0.9452	0.9950
$I_{cr,PCI}(x)$, in.^{4}	---	4046	4822
$I_{cr}(x)$, in.^{4}	---	3993	4760
$c_{cr}(x)$, in.	---	2.13	2.24
$e_{cr}(x)$, in.	---	16.936	18.51
$I_e(x)$, in.^{4}	20,985	14,436	20,299
$e_e(x)$, in.	5.48	11.30	13.77
$\phi(x) \times 10^{-6}$, 1/in.	−19.06	36.20	19.62
$\phi_{p,g}(x) \times 10^{-6}$, 1/in.	19.06	42.495	48.35
$\phi_{net}(x) \times 10^{-6}$, 1/in.	0	78.695	67.98‡
$\phi_D(x) \times 10^{-6}$, 1/in.	0	41.10	42.81
$\phi_L(x) \times 10^{-6}$, 1/in.	0	37.595	25.17§

*Loss of prestress in bond transfer length not accounted for

†Class T prestressed member since $f_r < f_b < 12\sqrt{f'_c} = 848.5$ psi

‡$\phi_{net}(0.5\ell) \approx 81.97 \times 10^{-6}$ 1/in. with parabolic approximation

§$\phi_L(0.5\ell) \approx 39.16 \times 10^{-6}$ 1/in. with parabolic approximation

Alternative trapezoidal approximation for net curvature and deflection calculations

Estimating deflection by approximating the distribution of net curvature with a trapezoidal curve as shown in Fig. A6 (corresponding to the shape for an elastic beam under two-point loading, assuming the loading points are located at 0.4ℓ from each support), gives

$\Delta_{net} = K_M \phi_{net}(0.4\ell)\ell^2 = 0.0983 \times 78.695 \times 10^{-6} \times (70 \times 12)^2 =$ 5.46 in.

where

$$K_M = \left[3 - 4\left(\frac{a}{\ell}\right)^2\right] / 24 = \left[3 - 4(0.4)^2\right] / 24 = 4.72/48 = 0.0983$$

$$\Delta_{i,L} = \Delta_{net} - \Delta_{i,D} = 5.46 - 3.15 = 2.31 \text{ in.}$$

$$\Delta_a = \Delta_{net} - \Delta_{p,g} = 5.46 - 3.40 = 2.06 \text{ in.}$$

These estimated values of 2.31 in. for $\Delta_{i,L}$ and 2.06 in. for Δ_a are closer to the integrated values of deflection (2.39 in. for $\Delta_{i,L}$ and 2.14 in. for Δ_a) but now underestimate deflection by 3 to 4%. Compare this with the estimate using a parabolic distribution of curvature, where deflections are overestimated by about 20 to 23%.

Further investigation with this type of tendon profile is needed for different ratios of service load to cracking load before definite recommendations can be made regarding the merits of each approximation.

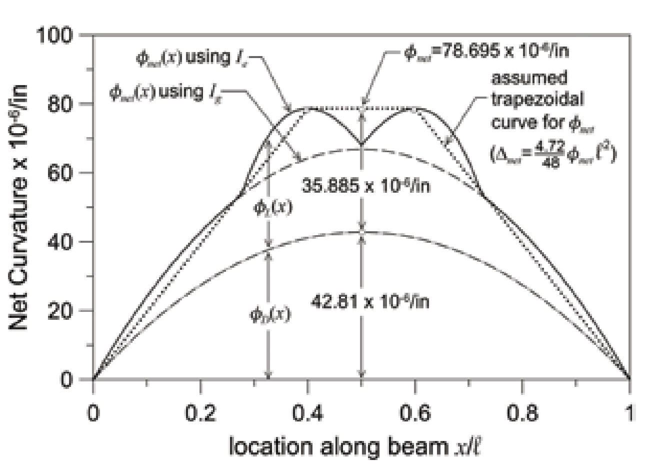

Fig. A6: Beam example for distribution of net curvature approximated with a trapezoidal curve

Aside 1: Location of Critical Section for Deflection Calculation

Determine the location for the maximum value of total stress f_b at the bottom (precompressed) tensile face of the prestressed beam (refer to Fig. A2).

The angle of inclination θ of the prestressing force given by

$$\theta = 2\left(e_{g,c} - e_{g,end}\right)/\ell$$

is used to obtain the eccentricity $e_g(x)$ along the beam span

$$e_g\left(x\right) = e_{g,end} + \theta x \text{ for } x \le \ell/2$$

For the bottom stress f_b in the section for the prestress force plus dead and live load (where compression is negative and tension is positive)

$$f_b\left(x\right) = -\frac{P_e}{A_g} - \frac{P_e e_g\left(x\right) y_{bot}}{I_g} + \frac{M\left(x\right) y_{bot}}{I_g}$$

where $M\left(x\right) = 4M_a\left[\left(x/\ell\right) - \left(x/\ell\right)^2\right]$ and $M_a = w\ell^2/8$ at midspan

Setting $\frac{d}{dx} f_b\left(x\right) = 0$ identifies the location of maximum stress for f_b, giving

$$x/\ell = 0.5 - P_e\theta\ell/\left(8M_a\right) = 0.5 - P_e\left(e_{g,c} - e_{g,end}\right)/\left(4M_a\right)$$

$x/\ell = 0.39$ for $P_e = 297.4$ kip, $\theta = 0.02005$ rads, $\ell = 70$ ft, and $M_a = 5718.3$ kip-in.

Similarly, the location for the maximum value of $M(x)/M_{cr}(x)$ occurs at

$$x/\ell = \sqrt{\omega^2 + \omega} - \omega, \text{ with}$$

$$\omega = \frac{e_{g,end} + I_g/\left(A_g y_{bot}\right) + f_r I_g/\left(P_e y_{bot}\right)}{2\left(e_{g,c} - e_{g,end}\right)} = 0.6361$$

to give $x/\ell = 0.384$, which is only a few percent different than the location for the maximum stress value f_b.

Aside 2: PCI Bilinear Load-Deflection Response Revisited

Example 5.8.3.1 from the PCI Design Handbook[12] computes deflection using a bilinear moment-deflection relationship as shown in Fig. A7. The PCI solution starts off by comparing the rupture modulus f_r with the computed stress at the bottom face f_b for the moment at 0.4ℓ (where tensile stresses for f_b are assumed to be greatest as discussed earlier). However, deflection is calculated at midspan (equivalent to using an approximation for the cracking moment at 0.5ℓ as shown in Fig. A7).

Stresses are computed at the bottom face for $x = 0.4\ell$. For the prestress load only:

$f_{pe}(0.4\ell) = 3710.75$ psi (C) from before.

For prestress plus the dead and live loads (total stress):

$$f_{b,tot}\left(0.4\ell\right) = -f_{pe}\left(0.4\ell\right) + \frac{M_D\left(0.4\ell\right) y_{bot}}{I_g} + \frac{M_L\left(0.4\ell\right) y_{bot}}{I_g} =$$

$$-3710.75 + \left(\frac{3513.9\left(17.15\right)}{20{,}985} + \frac{1975.7\left(17.15\right)}{20{,}985}\right) \times 1000 =$$

$$-3710.75 + 2871.74 + 1614.64 = 775.63 \text{ psi}\left(\text{T}\right) > f_r = 530 \text{ psi}$$

This beam is a Class T component since the total tensile stress $f_{b,tot} = 775.63$ psi (T) at the bottom face (for the prestress plus dead and live loads) is greater than f_r and less than $12\sqrt{f_c'} = 848.5$ psi. The stress $f_{b,p+D}$ from prestress plus dead load, which is equal to $-3710.75 + 2871.74 = -839.01 =$ 839.01psi (C), indicates the beam is uncracked for dead load only. The tensile stress $f_{b,L}$ from the live load alone equals 1614.64 psi (T).

That part of the live load w_{L1} needed to cause cracking at

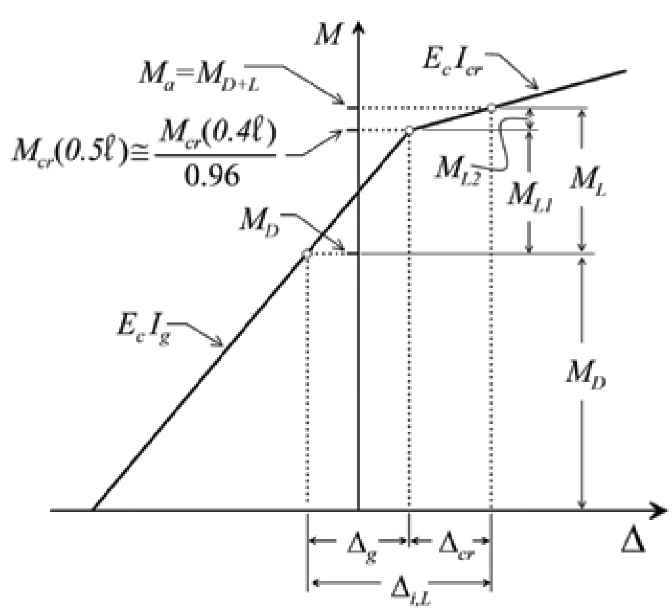

Fig. A7: Calculation of immediate deflection from live load using the PCI bilinear load-deflection response

0.4ℓ (for a bottom tensile stress of 530 psi) corresponds to a computed bottom stress from live load $f_{b,L1}$ = 839.01 + 530.0 = 1369.01 psi (T). This stress results from a portion of the total live load (280 lb/ft) as follows.

$$w_{L1} = \frac{f_{b,L1}}{f_{b,L}} w_L = \frac{1369.01}{1614.64} \times 280 = 237.40 \text{ lb/ft}$$

with a corresponding part of the live load moment M_{L1} at midspan.

$$M_{L1}(0.5\ell) = \frac{w_{L1}\ell^2}{8} = \frac{237.40(70)^2}{8} \times \frac{12}{1000} = 1744.9 \text{ kip-in.}$$

The stress $f_{b,L2} = f_{b,L} - f_{b,L1}$ from that part of the live load w_{L2} after cracking equals 1614.64 − 1369.01 = 245.63 psi (or $f_{b,tot} - f_r$ = 775.63 – 530 = 245.63 psi). Similarly

$$w_{L2} = \frac{f_{b,L2}}{f_{b,L}} w_L = \frac{245.63}{1614.64} \times 280 = 42.60 \text{ lb/ft}$$

$$M_{L2}(0.5\ell) = \frac{w_{L2}\ell^2}{8} = \frac{42.60(70)^2}{8} \times \frac{12}{1000} = 313.1 \text{ kip-in.}$$

Deflection is computed using the midspan (0.5ℓ) value of d_p = 20.75 in. for ρ_p = 1.836/(96 × 20.75) = 0.00092, to give $I_{cr} = n_p A_{ps} d_p^2 \left(1 - 1.6\sqrt{n_p \rho_p}\right) = 4822 \text{ in.}^4$

The deflection from live load up to cracking Δ_g (corresponding to deflection from the gross (uncracked) response)

$$\Delta_g = \frac{5}{48}\frac{M_{L1}\ell^2}{E_c I_g} = \frac{5}{48}\frac{(1744.9)(70 \times 12)^2}{(4074)(20,985)} = 1.50 \text{ in.}$$

and the deflection from live load after cracking Δ_{cr} (corresponding to deflection of the cracked response)

$$\Delta_{cr} = \frac{5}{48}\frac{M_{L2}\ell^2}{E_c I_{cr}} = \frac{5}{48}\frac{(313.1)(70 \times 12)^2}{(4074)(4822)} = 1.17 \text{ in.}$$

Total live load deflection $\Delta_{i,L} = \Delta_g + \Delta_{cr}$ = 1.50 + 1.17 = 2.67 in.

The procedure followed above for computing deflection from live load is equivalent to using a *fictitious* cracking moment at midspan based on the cracking moment computed at 0.4ℓ divided by 0.96 (assuming a parabolic curve for distribution of the moment along the span) as shown in Fig. A7.

$M_{cr}(0.4\ell) = 5189.0$ k-in. from before, and

$$M_{cr}(0.5\ell) \approx \frac{M_{cr}(0.4\ell)}{0.96} = \frac{5189.0}{0.96} = 5405.2 \text{ kip-in.}$$

to give

$$M_{L1} = M_{cr}(0.5\ell) - M_D(0.5\ell) = 5405.2 - 3660.3 = 1744.9 \text{ kip-in. as before, and}$$

$$M_{L2} = M_{D+L}(0.5\ell) - M_{cr}(0.5\ell) = 5718.3 - 5405.2 = 313.1 \text{ kip-in. as before.}$$

Computed values of deflection are slightly different from those in the PCI example[12] because of differences in the value used for E_c and roundoff error.

Table A2 provides a summary of calculated deflection values using the different procedures evaluated in this bonus example (with the values in brackets giving the percent difference compared to deflection computed by integrating curvature). Computed values of immediate deflection from live load range from 99 to 124% of the ACI CODE-318 deflection limit of $\ell/360$ = 2.33 in. depending on the procedure used. Comparison of results are specific to this example and can differ for other examples such as the rectangular beam example from this article.

Table A2:
Summary of calculated deflection values

Deflection	Δ_a, in.	$\Delta_{i,L}$, in.	$\Delta_{i,L}/\Delta_{all}$
Direct calculation using parabolic approximation for net curvature	2.625 (+23%)	2.88 (+20.5%)	1.24
Direct calculation using trapezoidal approximation for net curvature	2.06 (–4%)	2.31 (–3%)	0.99
Bilinear load-deflection response	---	2.67 (+12%)	1.15
Integration of curvature	2.14	2.39	1.03

$\Delta_{all} = \ell/360 = 2.33$ in. for immediate deflection from live load

Notation for Parts 1 to 5 of this article (including bonus deflection example)

A_b = area of reinforcing bar
A_g = area of gross (uncracked) concrete section
A_{ps} = area of prestressed longitudinal tension reinforcement
A_s = area of nonprestressed longitudinal tension reinforcement
A_s' = area of compression reinforcement
b = width of compression face of member
c_{cr} = distance from compression face to neutral axis of a fully cracked cross section
d = effective depth of tension reinforcement (distance from compression face to centroid of nonprestressed tension reinforcement)
d_p = effective depth of prestressed tension reinforcement
e = eccentricity of prestressing force relative to centroid of section
e_{cr} = eccentricity of prestressed reinforcement relative to centroid of fully cracked section ($= d_p - c_{cr}$)
e_e = effective eccentricity of prestressed reinforcement
e_g = eccentricity of prestressed reinforcement relative to centroid of gross (uncracked) concrete section
$e_{g,c}$ = eccentricity of prestressing force (for gross section) at center of span (midspan)
$e_{g,end}$ = eccentricity of prestressing force (for gross section) at end of span
e_{tr} = eccentricity of prestressed reinforcement relative to centroid of uncracked transformed section
E = elastic modulus
E_c = elastic modulus of concrete
E_p = elastic modulus of prestressing reinforcement
E_s = elastic modulus of nonprestressed reinforcing steel
f_b = calculated stress in bottom fiber of cross section (assuming uncracked)
$f_{b,L}$ = stress from service live load in bottom fiber of cross section
$f_{b,L1}$ = stress from that part of the service live load to cause cracking in bottom fiber of cross section
$f_{b,L2}$ = remaining part of stress from service live load after cracking in bottom fiber of cross section
$f_{b,p+D}$ = stress from prestress plus service dead load in bottom fiber of cross section
$f_{b,tot}$ = total stress (from prestress plus service dead and live load) in bottom fiber of cross section
f_c' = specified compressive strength of concrete
f_{cr} = reduced cracking strength equal to $(2/3)f_r$
f_{dc} = decompression stress (stress in prestressed reinforcement corresponding to zero stress in the concrete at the prestress level)
f_{pe} = compressive stress in concrete from effective prestress force at precompressed tensile face
f_{pu} = specified tensile strength of prestressing reinforcement
f_r = modulus of rupture of concrete
f_{se} = effective stress in prestressed reinforcement after allowance for all prestress losses
f_y = specified yield strength of nonprestressed reinforcing steel
h = member thickness or height
h_{min} = minimum member thickness or height
I = moment of inertia

I_{cr} = moment of inertia of cracked transformed section (fully cracked section for a prestressed member)
I'_{cr} = moment of inertia of partially cracked transformed section
I_e = effective moment of inertia
$I_{e,avg}$ = average or weighted average of effective moment of inertia for the member
$I_{e,D}$ = effective moment of inertia for the service dead load
$I_{e,D+L}$ = effective moment of inertia for the full (dead plus live) service load
$I_{e,m}$ = effective moment of inertia at midspan
I_{e1} = effective moment of inertia at end support 1 of continuous member (corresponding to moment M_1)
I_{e2} = effective moment of inertia at end support 2 of continuous member (corresponding to moment M_2)
I_g = moment of inertia of the gross (uncracked) concrete section (neglecting reinforcement)
I_{tr} = moment of inertia of the uncracked transformed section
k_{cr} = ratio of neutral axis depth of elastic cracked section to the effective depth
K = deflection coefficient for calculating deflection (K_M for load, K_p for prestressing)
ℓ = span length of member
ℓ_n = clear span of member
M = moment
M_a = maximum moment in member for service load stage at which deflection is calculated
M_{cr} = cracking moment
ΔM_{cr} = tension stiffening moment at cracking
M_{dec} = decompression moment (corresponding to zero stress at tension face of prestressed member)
M_D = dead load service moment
M_{D+L} = full (dead plus live load) service moment
M_L = live load service moment
M_{L1} = that part of the live load moment needed to cause cracking
M_{L2} = remaining part of live load moment after cracking (M_L - M_{L1})
$M_{L,sus}$ = sustained part of live load moment
M_m = moment at midspan
M_n = nominal flexural strength
M_o = static moment
M_{sus} = sustained moment
ΔM_{ts} = tension stiffening moment
M_u = ultimate (factored) moment
M_1 = intercept moment of shifted E_cI_{cr} response with uncracked E_cI_{tr} response (for prestressed member)
M_1 = moment at end support 1 of continuous member
M_2 = moment at end support 2 of continuous member
n_p = modular ratio (ratio of E_p to E_c)
P_e = effective prestress force
P_o = fictitious decompression (prestress) force
q = uniformly distributed area load (load per unit area)
q_a = uniformly distributed (dead plus live) service load (load per unit area)
q_{equiv} = fictitious (equivalent) uniformly distributed area load (for beams)
q_D = uniformly distributed dead load (load per unit area)
q_L = uniformly distributed live load (load per unit area)
q_{sus} = uniformly distributed sustained load (load per unit area)
w = uniformly distributed line load (load per unit length)
w_D = uniformly distributed dead load per unit length (w_{sw} + w_{sd})
w_L = uniformly distributed live load per unit length
w_{L1} = that part of the live load needed to cause cracking
w_{L2} = remaining part of the live load after cracking (w_L - w_{L1})
w_{sd} = superimposed dead load per unit length
w_{sw} = load from member self-weight (load per unit length)
y_t = distance from centroidal axis of gross (uncracked) section to tension face
y_{bot} = distance from bottom fiber to center of gravity of uncracked (gross) section
y_{top} = distance from top fiber to center of gravity of uncracked (gross) section
β_{ts} = tension stiffening factor

θ = angle of draped prestressing tendon
Δ = deflection
Δ_a = deflection at M_a
Δ_{all} = allowable deflection limit
Δ_{calc} = calculated deflection
Δ_{cr} = deflection at cracking
Δ_{cr} = deflection from live load after cracking (for cracked prestressed member)
Δ_{exp} = experimental deflection (including camber and member self-weight)
Δ_g = deflection from live load up to cracking (for cracked prestressed member)
Δ_i = immediate deflection
$\Delta_{i,D}$ = immediate deflection from dead service load
$\Delta_{i,D+L}$ = immediate deflection from full (dead plus live) service load
$\Delta_{i,L}$ = immediate deflection from live service load
$\Delta_{i,L(sus)}$ = immediate deflection from sustained part of the live load
$\Delta_{i,sus}$ = immediate deflection from sustained load (dead plus sustained part of live load)
Δ_{inc} = incremental deflection (occurring after attachment of nonstructural elements)
Δ_{net} = net deflection (dead plus live load deflection)
$\Delta_{p,g}$ = deflection (camber) from eccentric prestressing of gross (uncracked) member
λ = modification factor for lightweight concrete
λ_{cr} = reduction factor applied to cracking moment
λ_Δ = long-term deflection multiplier
ξ = time-dependent factor for sustained load
ρ = reinforcement ratio of tension reinforcement [= $A_s/(bd)$]
ρ_p = reinforcement ratio of prestressed reinforcement [= $A_{ps}/(bd_p)$]
ρ' = reinforcement ratio of compression reinforcement [= $A_s'/(bd)$]
ρ_b = balanced reinforcement ratio
ϕ = strength reduction factor (for strength design)
ϕ = curvature (M/EI)
ϕ_a = curvature at full (dead plus live) service load moment M_a (including curvature from prestressing when applicable)
ϕ_D = curvature from dead load
ϕ_L = curvature from live load
ϕ_m = curvature at midspan of simply supported and continuous members
ϕ_{net} = net curvature relative to uncracked curvature from prestressing (= $\phi_D + \phi_L$)
ϕ_{p+D} = curvature of gross (uncracked) section from prestressing force plus service dead load
$\phi_{p,cr}$ = curvature of cracked section from prestressing force
ϕ_{pe} = effective curvature from prestressing force
$\phi_{p,g}$ = curvature of gross (uncracked) section from prestressing force
$\phi_{p,tr}$ = curvature of uncracked transformed section from prestressing force
ϕ_1 = curvature at end support 1 of continuous member
ϕ_2 = curvature at end support 2 of continuous member

04

Cálculo de Deflexiones Utilizando el CÓDIGO-318-19 de ACI y Otros Más, Parte 5

Extensión propuesta para el concreto presforzado.

Por Peter H. Bischoff, Wassim Nasreddine y Hani Nassif

Partes 1 a 4 de esta serie de artículos[1-4] introducen y evalúan la nueva expresión para I_e adoptada primero por el CÓDIGO ACI-318-19[5] para calcular la deflexión del concreto reforzado (no presforzado). La expresión revisada para I_e no corresponde a miembros de concreto presforzados agrietados y el CÓDIGO ACI-318-19 utiliza el enfoque desarrollado por Branson[6] para este tipo de miembros.

El trabajo de Bischoff et al.[7] propone extender el enfoque del CÓDIGO ACI-318-19 para el concreto reforzado, de manera que incluya concreto presforzado. El planteamiento propuesto resumido en la Fig. 1, se desarrolló para calcular la deflexión inmediata de miembros presforzados Clase T y Clase C que se agrietan bajo carga de servicio (consulte el CÓDIGO-318 de ACI, Sección 24.5.2, para la clasificación de miembros presforzados). En este enfoque, la deformación por la fuerza de presfuerzo excéntrica (calculada mediante el uso de una excentricidad efectiva e_e y momento de inercia efectivo I_e) se resta de la deformación por la carga (calculada utilizando I_e). Esto se parece mucho al procedimiento utilizado para calcular la deflexión de un miembro presforzado no agrietado, en el que e_g (la excentricidad de la fuerza de presfuerzo relativa al centroide de la sección bruta [no agrietada]) e I_g se utilizan para calcular la contraflecha, además I_g se utiliza para calcular la deflexión debida a la carga (pero con una diferencia para un miembro agrietado, tal como se observa adelante).

Si bien la curvatura de un miembro presforzado agrietado se obtiene al restar la curvatura efectiva provocada por la fuerza de presfuerzo excéntrica de la curvatura causada por la carga, el cálculo directo de la deflexión se basa conservadoramente en la curvatura neta[7], tal como se demuestra con un ejemplo posterior en este artículo. Para un miembro o miembros continuos con excentricidad variable del presfuerzo, podría ser favorable calcular la deflexión integrando la curvatura. Calcular la deflexión de forma directa (sin integración) también se ve afectada por el tipo de carga. En el Apéndice está disponible un ejemplo extra para un miembro con excentricidad variable, al que se puede acceder en la versión en línea de este artículo en *www.concreteinternational.com.*

$$I_e = I_g \quad \text{y} \quad e_e = e_g \text{ para } M_a \le \lambda_{cr} M_{cr}$$

Para $M_a > \lambda_{cr} M_{cr}$

$$I_e = \frac{I_{cr}}{1 - \left(\dfrac{\lambda_{cr} M_{cr}}{M_a}\right)^2 \left(1 - \dfrac{I_{cr}}{I_g}\right)}$$

$$e_e = \left(\frac{\lambda_{cr} M_{cr}}{M_a}\right)\left(\frac{I_e}{I_g}\right) e_g + \left[1 - \left(\frac{\lambda_{cr} M_{cr}}{M_a}\right)\right]\left(\frac{I_e}{I_{cr}}\right) e_{cr}$$

$$M_{cr} = \left(f_r + f_{pe}\right) I_g / y_t$$

$$\lambda_{cr} = \left(\frac{2}{3}\right) + \left(\frac{\rho_p}{\rho + \rho_p}\right)\left(\frac{1}{3}\right)$$

Fig. 1: Revisión propuesta para el Código ACI-318-19, Sección 24.2.3.9

Resumen de las Partes del Artículo	
Parte 1	Introducción al cálculo de deflexiones inmediatas y dependientes del tiempo
Parte 2	Nueva Expresión para I_e y Razones del Cambio
Parte 3	Impacto de los Cambios Realizados
Parte 4	Ejemplo de Deflexión – Losa Continua
Parte 5	Extensión Propuesta para Concreto Presforzado

Comportamiento del Concreto Presforzado

La Figura 2 ilustra el efecto del presforzado en la relación momento-curvatura para los miembros a flexión de concreto. El presforzado excéntrico incrementa el momento de agrietamiento y causa una deflexión ascendente inicial (contraflecha) para dar una respuesta más rígida en cargas de servicio. La fuerza de presfuerzo axial también da por resultado una sección parcialmente agrietada con una respuesta $E_cI'_{cr}$ no lineal que converge gradualmente (bajo carga en incremento) con la respuesta E_cI_{cr} que corresponde a una sección completamente agrietada (no presforzada). Más importante aún, la respuesta E_cI_{cr} agrietada se compensa por la respuesta E_cI_{cr} no agrietada (donde el momento M_I identifica el punto de intersección de la respuesta E_cI_{tr} y cambia la respuesta E_cI_{cr}). La respuesta E_cI_{cr} se muestra en la Fig. 2 como justo debajo del momento de agrietamiento M_{cr}, pero puede encontrarse sobre M_{cr} para niveles más altos de presfuerzo.[8]

El cálculo de la deflexión se simplifica utilizando la respuesta E_cI_{cr} en lugar de $E_cI'_{cr}$.[7,9] Esto evita la dificultad de localizar el eje neutro y después la ubicación del centroide que no coincide con el eje neutro para una sección parcialmente agrietada. Otras simplificaciones incluyen aproximar el momento de inercia I_{tr} no agrietado con un momento de inercia bruto I_g y utilizar la fuerza de presfuerzo efectiva P_e en lugar de la fuerza de descompresión ficticia (presfuerzo) $P_o = f_{dc}A_{ps}$ descrita por Nilson.[10] La fuerza de presfuerzo se mueve hasta el centroide para análisis, lo que da por resultado un momento de presfuerzo excéntrico $P_oe_{cr} \approx P_ee_{cr}$, donde e_{cr} es la excentricidad del acero de presfuerzo relativo al centroide de la sección agrietada (ubicada en el eje neutro para la sección completamente agrietada).

El esfuerzo de descompresión f_{dc} se define como el esfuerzo en el tendón correspondiente a esfuerzo cero en el concreto a nivel de los tendones presforzados y A_{ps} es el área de refuerzo de tensión longitudinal. La fuerza de presfuerzo efectivo es $P_e = f_{se}A_{ps}$, donde f_{se} es el esfuerzo efectivo en el refuerzo presforzado después de todas las pérdidas, incluyendo contracción y el flujo plastico. El momento de más agrietamiento relacionado con el presfuerzo es $M_{cr} = (f_r + f_{pe})\, I_g/y_t$, donde f_{pe} es el esfuerzo de compresión en el concreto en la cara a tensión precomprimida que es el resultado de la fuerza de presfuerzo efectivo P_e que actúa sobre la sección deforme y por tanto, también responde por las pérdidas de flujo plastico y contracción.

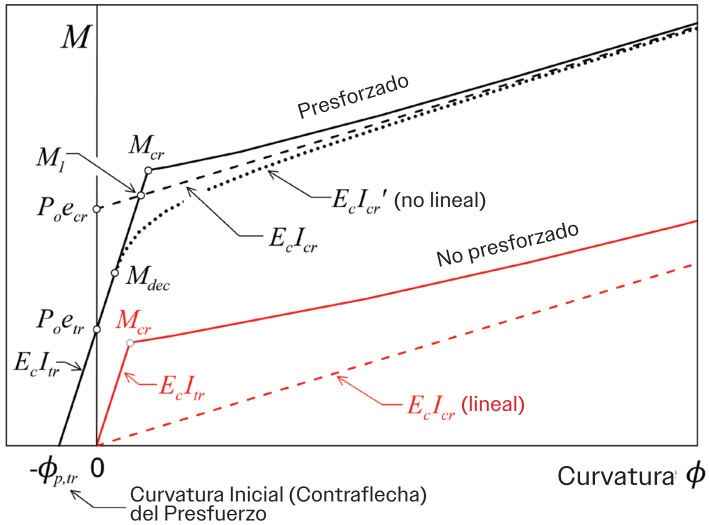

Fig. 2: Gráficas comparativas de relaciones momento-curvatura para miembros a flexión presforzados y reforzados (no presforzados)

Extensión del Modelo a Concreto Presforzado

La deformación de un miembro de concreto presforzado agrietado se modela agregando un momento de endurecimiento por tensión $\Delta M_{ts} = \beta_{ts}\Delta M_{cr} \leq \Delta M_{cr}$ en la respuesta E_cI_{cr} agrietada, tal como se ilustra en la Fig. 3.[7,9] Esto es similar al planteamiento utilizado para concreto reforzado (no presforzado) descrito en la Parte 2 de la serie de artículos,[2] a excepción de que la respuesta E_cI_{cr} se cambió hacia arriba en relación con la respuesta E_cI_{tr} no agrietada. El desarrollo del modelo para concreto presforzado replica los pasos tomados en la Parte 2 de la serie de artículos[2] para concreto reforzado.

El momento M_a para la curvatura correspondiente a ϕ_a se define como

$$M_a = E_cI_{cr}\left(\phi_a + \phi_{p,cr}\right) + \beta_{ts}\Delta M_{cr} \qquad (1a)$$

El reordenamiento de los términos conduce a

$$\phi_a = \frac{M_a}{E_cI_{cr}}\left[1-\beta_{ts}\left(\frac{\Delta M_{cr}}{M_a}\right)\right] - \phi_{p,cr} \qquad (1b)$$

Sustituyendo

$$\Delta M_{cr} = M_{cr}\left(1 - I_{cr}/I_{tr}\right) - E_cI_{cr}\left(\phi_{p,cr} - \phi_{p,tr}\right)$$

en la ecuación (1b) da

$$\phi_a = \frac{M_a}{E_cI_{cr}}\left[1-\beta_{ts}\left(\frac{M_{cr}}{M_a}\right)\left(1-\frac{I_{cr}}{I_{tr}}\right)\right] - \left[\beta_{ts}\phi_{p,tr} + (1-\beta_{ts})\phi_{p,cr}\right] \qquad (1c)$$

lo que conduce a la curvatura $\phi_a = M_a/(E_cI_e) - \phi_{pe}$ para un momento de inercia I_e efectivo y una curvatura efectiva de presfuerzo ϕ_{pe}, se define como

$$I_e = \frac{I_{cr}}{1-\beta_{ts}\left(\frac{M_{cr}}{M_a}\right)\left(1-\frac{I_{cr}}{I_{tr}}\right)} \qquad (2a)$$

y

$$\phi_{pe} = \beta_{ts}\phi_{p,tr} + (1-\beta_{ts})\phi_{p,cr} \qquad (2b)$$

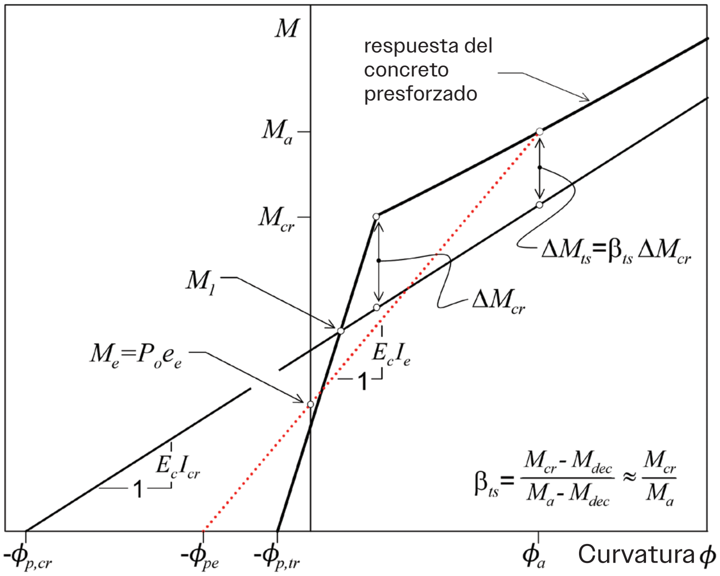

Fig. 3 Respuesta del modelo del miembro presforzado con endurecimiento por tensión

La curvatura del presfuerzo de una sección no agrietada $\phi_{p,tr}$, se da por $\phi_{p,tr} = P_oe_{tr}(E_cI_{tr})$, y la curvatura del presfuerzo de una sección completamente agrietada se da por $\phi_{p,cr} = P_oe_{cr}/(E_cI_{cr})$· ΔM_{ts} disminuye con la carga mayor después del agrietamiento, utilizando un factor de endurecimiento por tensión asumido $\beta_{ts} = M_{cr}/M_a$ que se sustituye en la ecuación (2a) y (2b). Más, los términos para la sección transformada no agrietada (I_{tr}, $\phi_{p,tr}$, y e_{tr}) se transforman con los términos para una sección bruta (no agrietada) (I_g, $\phi_{p,g}$, y e_g) para dar expresiones de diseño simplificadas para I_e y ϕ_{pe}.

$$I_e=\frac{I_{cr}}{1-\left(\frac{M_{cr}}{M_a}\right)^2\left(1-\frac{I_{cr}}{I_g}\right)} \tag{3a}$$

$$\phi_{pe}=\left(\frac{M_{cr}}{M_a}\right)\phi_{p,g}+\left[1-\left(\frac{M_{cr}}{M_a}\right)\right]\phi_{p,cr} \tag{3b}$$

Se toma un paso final al establecer $P_oe_e = (E_cI_e)\phi_{pe}$ para definir una excentricidad efectiva e_e. Haciendo otra simplificación aproximando P_o con P_e (básicamente calculando el esfuerzo de descompresión f_{dc} con el presfuerzo efectivo f_{se}), donde $\phi_{p,g} = P_ee_g(E_cI_g)$ y $\phi_{p,cr} = P_ee_{cr}/(E_cI_{cr})$, conduce a

$$e_e=\left(\frac{M_{cr}}{M_a}\right)\left(\frac{I_e}{I_g}\right)e_g+\left[1-\left(\frac{M_{cr}}{M_a}\right)\right]\left(\frac{I_e}{I_{cr}}\right)e_{cr}$$

Entonces la curvatura se calcula como $\phi_a = (M_a - P_ee_e)/(E_cI_e)$. La Figura 4 ilustra la respuesta del miembro calculada cuando la respuesta E_cI_{cr} se encuentra ya sea debajo o sobre el momento de agrietamiento.

Restricción de la Contracción por Refuerzo no Presforzado

El momento de agrietamiento $M_{cr}=(f_r+f_{pe})I_g/y_t$ no se reduce para un miembro completamente presforzado (FP [por sus iniciales en inglés]) (donde la sección no incluye refuerzo no presforzado). Esto se debe a que la contracción y el flujo plastico ya se tomaron en consideración con el esfuerzo efectivo f_{se} en el acero de presfuerzo utilizado para establecer la fuerza de presfuerzo efectiva P_e y el esfuerzo de compresión subsecuente f_{pe} en la cara a tensión precomprimida (que a su vez se utiliza para calcular M_{cr}). No obstante, se necesita un momento de agrietamiento reducido $\lambda_{cr}M_{cr}$ para un miembro presforzado reforzado con refuerzo adicional no presforzado (definido como parcialmente presforzado [PP] en este artículo) para responder por los esfuerzos de tensión que se desarrollan en el concreto por la restricción a la contracción mediante el refuerzo no presforzado.[11] El factor de reducción

$$\lambda_{cr}=\left(\frac{2}{3}\right)+\left(\frac{\rho_p}{\rho+\rho_p}\right)\left(\frac{1}{3}\right)$$

varia entre 2/3 para un miembro de concreto reforzado (no presofrzado) (idéntico al Código ACI 318-19 para concreto no presforzado) y 1 para un miembro FP. La substitución del momento de agrietamiento reducido en la ecuación (3) entonces da

$$I_e=\frac{I_{cr}}{1-\left(\frac{\lambda_{cr}M_{cr}}{M_a}\right)^2\left(1-\frac{I_{cr}}{I_g}\right)} \tag{4a}$$

$$\phi_{pe}=\left(\frac{\lambda_{cr}M_{cr}}{M_a}\right)\phi_{p,g}+\left[1-\left(\frac{\lambda_{cr}M_{cr}}{M_a}\right)\right]\phi_{p,cr} \tag{4b}$$

$$e_e=\left(\frac{\lambda_{cr}M_{cr}}{M_a}\right)\left(\frac{I_e}{I_g}\right)e_g+\left[1-\left(\frac{\lambda_{cr}M_{cr}}{M_a}\right)\right]\left(\frac{I_e}{I_{cr}}\right)e_{cr} \tag{4c}$$

Las propiedades de la sección bruta (I_g, $\phi_{p,g}$, e_g) se utilizan para un miembro no agrietado cuando $M_a \leq \lambda_{cr}M_{cr}$.

Evaluación

Los detalles completos sobre el nivel de precisión de este planteamiento basados en la comparación con una extensa base de datos de pruebas que utiliza los resultados de 180 vigas de 23 estudios se proporcionan en otra parte.[7] Estas vigas tenían formas rectangulares, de una sola t o tenían forma de I; estaban soportadas de manera sencilla; tenían un perfil de tendón recto presforzado con excentricidad constante y estaban sujetas a dos cargas de puntos colocados simétricamente.[11] La Figura 5 muestra una amplia variabilidad de resultados de estas pruebas, tal como se espera, donde las deflexiones experimentales Δ_{exp} (incluyendo peralte y peso propio del miembro) se comparan con los valores calculados Δ_{calc} utilizando el procedimiento descrito en el ejemplo de deflexión. La deflexión se sobreestima por una cantidad moderada en promedio, con una relación de predicción de deflexión media ($\Delta_{calc}/\Delta_{exp}$) igual a 1.24 cuando los valores de deflexión se calculan directamente (basándose en los cálculos de curvatura neta, tal como se muestran en el ejemplo). La curvatura de integración (basada en I_e y en e_e calculada en cada sección junto con el tramo del miembro) disminuye la relación media $\Delta_{calc}/\Delta_{exp}$ a un valor de 1.06. Al utilizar la fuerza de presfuerzo de descompresión P_o y las propiedades de la sección transformada no agrietada para determinar M_{cr}, I_e, y e_e se mejora aún más la predicción de deflexión.[7]

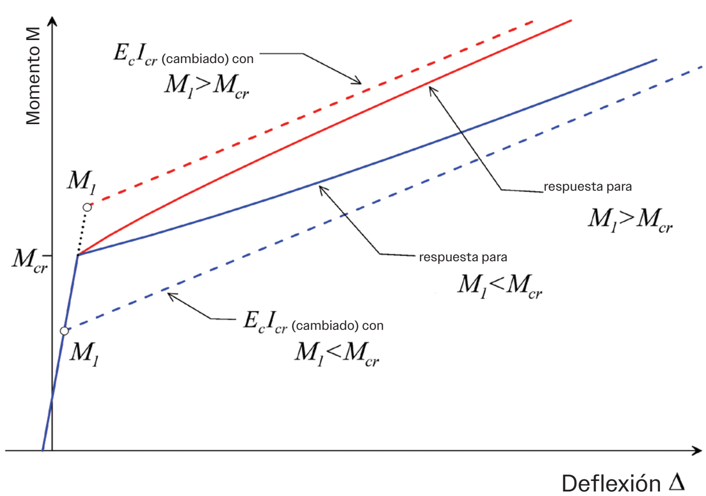

Fig. 4: Opciones de respuesta presforzada calculada.

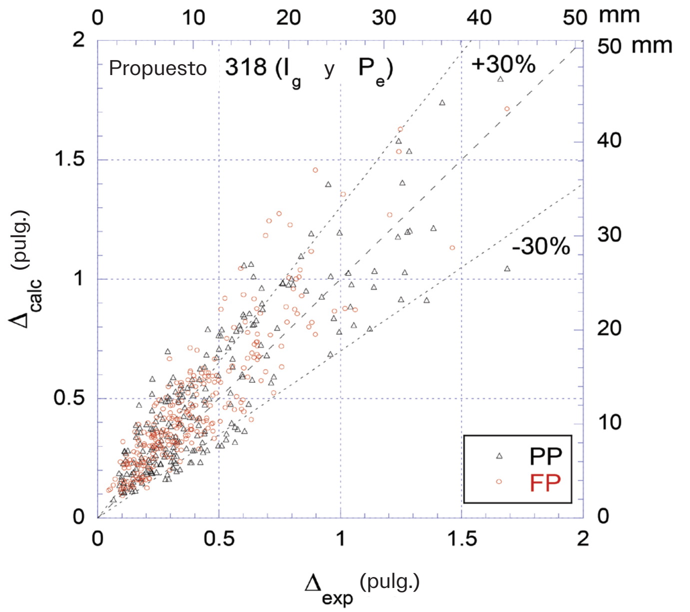

Fig. 5: Calculado versus deflexiones experimentales para vigas completamente presforzadas (FP) y parcialmente presforzadas (PP) *(utilizando la base de datos compilada en la Referencia 11)*

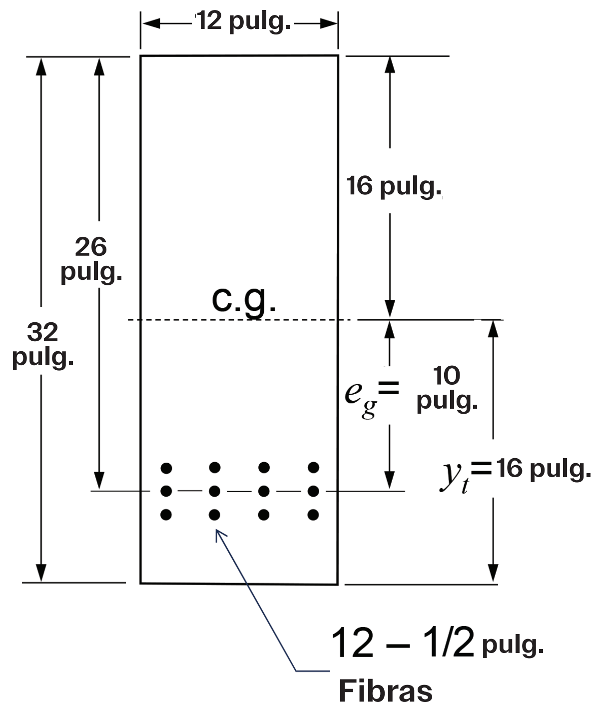

Fig. 6: Detalles del ejemplo de viga presforzada.

Ejemplo de Deflexión Presforzada

El ejemplo 5.2.2.5 tomado del PCI Design Handbook 2020[12] y basado en el Ejemplo 1 del documento PCI de Mast[13] se utiliza para demostrar el planteamiento propuesto para calcular la deflexión inmediata de una viga presforzada soportada de forma sencilla agrietada bajo carga de servicio. La viga presforzada es rectangular, tal como se ilustra en la Fig. 6 y presforzada con doce fibras 270K de ½ pulgada de diámetro colocadas a una profundidad efectiva d_p = 26 pulgadas. El tramo l = 40 pies, f'_c = 6 000 psi, y $E_c = 57\,000\sqrt{f'_c}$ = 4 415 ksi para dar $n_p = E_p/E_c$ = 6.46 (asumiendo E_p = 28 500 ksi).

Las cargas y los momentos a mitad de vano son los siguientes:

Peso propio = 150 lb/pies^3 x (12/12) pies x (32/12)pies ÷ 1 000 =

0.40 kip/pies

Carga muerta superimpuesta = 1.0 kp/pies

Carga muerta total = 1.4 kp/pies

Carga viva = 1.25 kip/pies

M_D = 1.4 x 40^2/8 = 280 kip-pies = 3360 kip-pulg.

M_L = 1.25 x 40^2/8 = 250 kip-pies = 3000 kip-pulg.

$M_a = M_D + M_L$ = 530 kip-pies = 6360 kip-pulg.

Los detalles de la fuerza de presfuerzo son los siguientes:

A_{ps} = 12 x 0.153 = 1.836 pulg.^{2}

$p_p = A_{ps}(bd_p)$ = 1.836/(12 x 26) = 0.0059

(más p = 0 porque no hay refuerzo presforzado)

f_{pu} = 270 ksi

Nivel de presfuerzo inicial = 0.75f_{pu} y pérdida calculada de 20% da f_{se} = (1 – 0.20)(0.75)(270) = 162.0 ksi

P_e = 1.836 x 162.0 = 297.4 kip

Las propiedades de la sección son las siguientes:

A_g = 384 pulg.^{2} e I_g = 32 768 pulg^4

y_t = 16 pulg. y e_g = 26 – 16 = 10 pulg. (ver Fig. 6)

$f_{pe} = P_e/A_g + (P_e \times e_g)y_t/I_g$ = 297.4/384 + (297.4 x 10) x

16/32 768 = 2.227 ksi

$f_r = 7.5\sqrt{f'_c} = 7.5\sqrt{6000}$ = 581 psi

$M_{cr} = (f_r + f_{pe})\,I_g/y_t$ = (0.581 + 2.227) 32 768/16 = 5 750 kip-pulg.

λ_{cr} = (2/3) * [0.0059/(0 + 0.0059)](1/3) = 1.0 y

$\lambda_{cr}M_{cr}$ = 5750 kip-pulg.

$n_p p_p$ = 6.46 x 0.0059 = 0.038

$$k_{cr} = \sqrt{\left(n_p\rho_p\right)^2 + 2\left(n_p\rho_p\right)} - \left(n_p\rho_p\right) =$$
$$\sqrt{(0.038)^2 + 2\times 0.038} - 0.038 = 0.240$$

$c_{cr} = k_{cr} \times d_p = 0.240 \times 26 = 6.24$ in. y $e_{cr} = 26 - 6.24 =$ 19.76 in.

(el centroide está ubicado en el eje neutral porque la sección está completamente agrietada.

$$I_{cr} = b(c_{cr})^3/3 + n_pA_{ps}\,(d_p - c_{cr})^2 =$$
$$12 \times (6.24)^3/3 + 6.46 \times 1.836 \times (26 - 6.24)^2 = 5\,603 \text{ pulg.}^4$$

Utilizando la aproximación PCI[12] para

$$I_{cr} = n_pA_{ps}d_p^{\,2}\left(1 - 1.6\sqrt{n_p\rho_p}\right)$$

$$I_{cr} = 6.46 \times 1.836 \times 26^2 \times \left(1 - 1.6\sqrt{0.038}\right) = 5517 \text{ in.}^4$$

Esta aproximación funciona razonablemente bien para p_p hasta más o menos 0.5% pero puede subestimar I_{cr} significativamente a relaciones de refuerzo más altas.[11]

Los cálculos de deflexión son de la siguiente forma:

La sección está agrietada bajo carga muerta completa más carga de servicio viva con

$$M_a = 6360 > \lambda_{cr}M_{cr} = 5750 \text{ kip-in.}$$
$$\lambda_{cr}M_{cr}/M_a = 0.904$$

$$I_e = \frac{5603}{1 - (0.904)^2\left(1 - 5603/32,768\right)} = 17,373$$

$$e_e = 0.904 \times \left(\frac{17,373}{32,768}\right) \times 10 + (1 - 0.904) \times \left(\frac{17,373}{5603}\right) \times 19.76 =$$

10.67

La curvatura ϕ_a en M_a se calcula como

$$\phi_a = M_a/(E_cI_e) - P_e \times e_e/(E_cI_e) = (M_a - P_e \times e_e)/(E_cI_e) =$$
$$(6360 - 297.4 \times 10.67)/(4415 \times 17,373) = 41.55 \times 10^{-6}\ 1/$$

Al referirnos a la Fig. 7, la curvatura neta $\phi_{neta} = \phi_a + \phi_{p,g} = \phi_D + \phi_L$

con $\phi_{p,g} = P_e \times e_g/(E_c I_g)$ = 297.4 x 10/(4 415 x 32 768) = 20.56 x 10^{-6} 1/pulg.

y $\phi_D = M_D(E_c I_g)$ = 3 360/(4 415 x 32 768) =23.22 x 10^{-6} 1/pulg.

$\therefore \phi_{neta}$ = (41.55 + 20.56) x 10^{-6} = 62.11 x 10^{-6} 1/pulg.

y $\phi_L = \phi_{neta} - \phi_D$ = (62.11 – 23.22) x 10^{-6} = 38.89 x 10^{-6} 1/pulg.

Deflexión neta $\Delta_{neta} = K_M \phi_{neta} \ell^2$ (con K_M = 5/48 para una distribución parabólica asumida de curvatura tal como se ilustra en la Figura 7.

Δ_{neta} = 5/48 x 62.11 x $(40 \times 12)^2$ x 10^{-6} = 1.491 pulg.

$\Delta_a = \Delta_{neta} - \Delta_{p,g}$ = 1.491 – 0.592 = 0.899 pulg.

con $\Delta_{p,g} = K_p \phi_{p,g} \ell^2$ = (1/8) x 20.56 x $(40 \times 12)^2$ x 10^{-6} = 0.592 pulg. K_p = 1/8 para un miembro con soporte sencillo con tendones rectos que tengan excentricidad constante.

Deflexión de carga viva $\Delta_{i,L} = \Delta_{neta} - \Delta_{i,D}$ con $\Delta_{i,D} = (5/48)\,\phi_D \ell^2$.

$\Delta_{i,D}$ = (5/48) x (23.22 x 10^{-6}) x $(40 \times 12)^2$ = 0.557 in.

y $\Delta_{i,L}$ = 1.491 – 0.557 = 0.934 pulg. Alternativamente,

$$\Delta_{i,L} = K_M \phi_L \ell^2 = \left(\frac{5}{48}\right) \times \left(38.89 \times 10^{-6}\right) \times \left(40 \times 12\right)^2 = 0.933 \approx 0.934 \text{ in.}$$

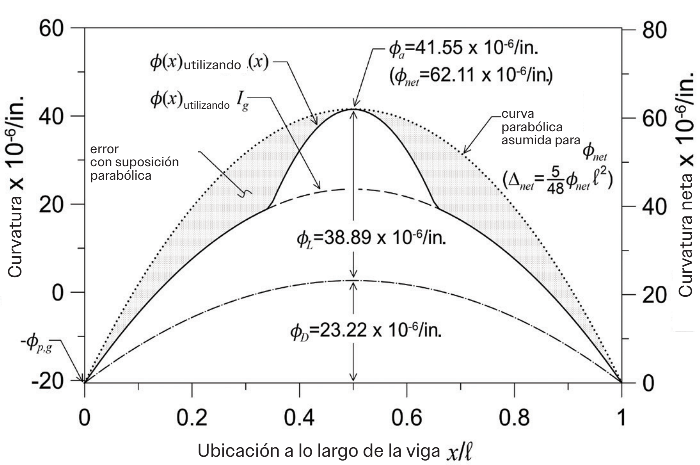

Fig. 7: Distribución de curvatura para ejemplo de viga.

El valor estimado de $\Delta_{i,L}$ = 0.934 pulg. sobreestima la deflexión de carga viva en 36% en comparación con un valor de 0.688 pulg. obtenido al integrar la curvatura, mientras que el valor para Δ_a = 0.899 pulg. sobreestima la deflexión en aproximadamente la misma cantidad en comparación con el valor de 0.653 pulg. cuando la curvatura está integrada. El área sombreada en la Fig. 7 representa el error al calcular la deflexión con la curvatura neta aproximada por una curva parabólica (asumiendo que la carga se distribuye de manera uniforme).

Aproximar la curvatura neta con una respuesta de distribución lineal (de forma triangular con ϕ_{neta} = 62.11 x 10-6 1/pulg. en el ápice ubicado a la mitad del vano) da valores de $\Delta_{i,L}$ = 0.635 pulg. y Δ_a = 0.600 pulg., que subestima la deflexión en aproximadamente 8% en cada caso, en comparación con integrar la curvatura.

La comparación también puede hacerse con el planteamiento más exacto basándose en P_o y las propiedades de la sección transformada no agrietada (I_{tr}, $\Delta_{p,tr}$, y e_{tr}) utilizadas para determinar M_{cr}, I_e, y e_e.

El esfuerzo de descompresión

$$f_{dc} = f_{se} + n_p \left(\frac{P_e}{A_g} + \frac{P_e \left(e_g\right)^2}{I_g} \right) = 172.9$$

y la fuerza de presfuerzo de descompresión $P_o = f_{dc} \times A_{ps}$ = 317.4 kip para dar un momento de agrietamiento más alto M_{cr} = 6 065 kip-pulg. (que actúa sobre la sesión transformada no agrietada). El momento de agrietamiento más alto disminuye considerablemente la deflexión calculada de la carga viva (de 0.934 pulg. a 0.690 pulg. utilizando la aproximación parabólica para la curvatura neta) debido a la proximidad más cercana del momento de carga de servicio M_a = 6 360 kip-pulg. al valor mayor del momento de agrietamiento (incrementando de 5 750 a 6 065 kip-pulg.). Los valores calculados de deflexión de carga viva varían entre 48 y 70% del límite del Código-318 de ACI de ℓ/360 = 1.33 pulg. para este ejemplo, dependiendo del curso en el procedimiento utilizado para calcular la deflexión.

Completamente presforzado (FP): miembro presforzado únicamente con refuerzo presforzado

Parcialmente presforzado (PP): miembro presforzado con refuerzo presforzado y no presforzado

Resumen

El planeamiento del Código-318-19 de ACI para calcular la deflexión inmediata del concreto reforzado (no presforzado) se amplía para incluir concreto presforzado cargado sobre el momento de agrietamiento (miembros presforzados Clase T y Clase C). Se utiliza un modelo mecánico racional como la base para agregar un componente de endurecimiento por tensión (en este momento de caso) en la respuesta E_cI_{cr} agrietada que se cambia hacia arriba en relación con la respuesta E_cI_g no agrietada debido a la fuerza de presfuerzo excéntrica. El enfoque propuesto resumido en la Fig. 1 para concreto presforzado incluye un momento efectivo de inercia Ie y excentricidad efectiva e_e de la fuerza de presfuerzo cuando el miembro se agrieta. I_g y e_g se utilizan para un miembro no agrietado. El momento de agrietamiento se reduce con un factor de reducción λ_{cr} para responder por los esfuerzos de tensión que se desarrollan en el concreto por la restricción a la contracción por el refuerzo no presforzado cuando está presente. Los procedimientos están presentes para calcular la deflexión directamente basándose en la curvatura neta (utilizando un valor uniforme asumido de I_e y e_e en la sección crítica) y comparado con la deflexión calculada al integrar la curvatura (utilizando I_e y e_e calculados en cada sección a lo largo del vano del miembro). La respuesta de carga-deflexión bilineal PCI también se considera en el ejemplo extra.

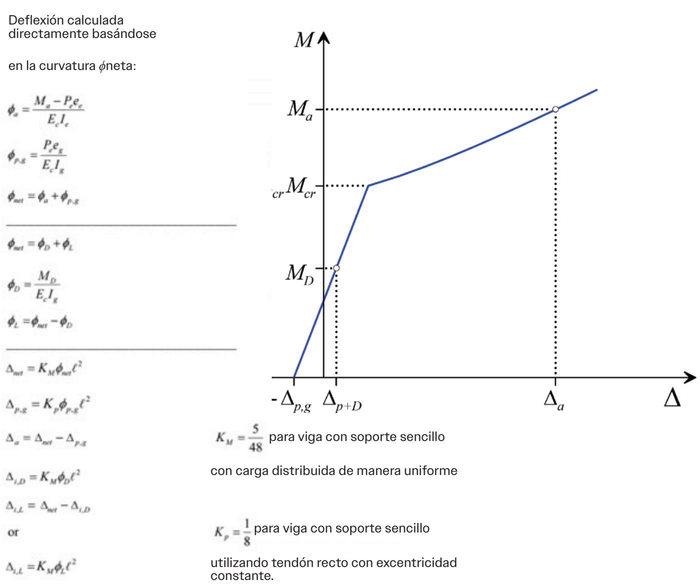

Reconocimientos

Se agradecen mucho los comentarios y sugerencias esclarecedores de Rex Donahey durante la redacción de esta serie de artículos (Partes 1 a 5).

Referencias

1. Bishoff, P.H., "Computing Deflections Using ACI CODE-318-19 AND Beyond, Part 1,"Concrete International, V.47, No. 2, Feb. 2025, pp. 47-50.
2. Bishoff, P.H., "Computing Deflections Using ACI CODE-318-19 AND Beyond, Part 2,"Concrete International, V.47, No. 3, Mar. 2025, pp. 51-54.
3. Bishoff, P.H., "Computing Deflections Using ACI CODE-318-19 AND Beyond, Part 3,"Concrete International, V.47, No. 4, Apr. 2025, pp. 47-50.
4. Bishoff, P.H., "Computing Deflections Using ACI CODE-318-19 AND Beyond, Part 4,"Concrete International, V.47, No. 5, May 2025, pp. 62-65.
5. ACI Committee 318, "Building Code Requirements for Structural Concrete (ACI 318-19) and Commentary (ACI 318R-19)," American Concrete Institute, Farmington Hills, MI, 2019, 624 pp.
6. Branson, D.E., Deformation of Concrete Structures, McGraw-Hill, New York, NY, 1977, 546 pp.
7. Bishoff, P.H.; Nasreddine, W.; and Nassif, H., "Proposed ACI 318 Equations for Immediate Deflection of Prestressed Concrete Members," ACI Structural Journal, V. 122, No. 6, Nov. 2025, pp. 127-139.
8. Bishoff, P.H.; Naito, C.J.; and Ingaglio, J.P., "Immediate Deflection of Partially Prestressed Concrete Flexural Members," ACI Structural Journal, V. 115, No. 6, Nov. 2018, pp. 1683-1693.
9. Bishoff, P.H.; "Deformation Model for Reinforced and Cracked Prestressed Concrete," ACI Structural Journal, V. 119, No. 1, Jan. 2022, pp. 243-254.
10. Nilson, A.H., "Flexural Stresses After Cracking in Partially Prestressed Beams," PCI Journal, V. 21, No. 4, July-Aug. 1976, pp. 72-81.
11. Nasreddine, W.; Obeidah, A.; Bishoff, P.H.; and Nassif, H., "Assessment of Deflection Prediction Models for Cracked Prestressed Concrete Beams," ACI Structural Journal, V. 120, No. 6, Nov. 2023, pp. 167-179.
12. PCI, PCI Design Handbook: Precast and Prestressed Concrete, seventh edition, Precast/Prestressed Concrete Institute, Chicago, IL, 2010, 804 pp.
13. Mast, R.F., "Analysis of Cracked Prestressed Concrete Sections: A Practical Approach," PCI Journal, V. 43, No. 4, July-Aug. 1998, pp. 80-91.

Recibido y revisado de conformidad con las políticas de publicación del Instituto.

Peter H. Bishoff, FACI, es Catedrático Emérito en Ingeniería Civil en la Universidad de New Brunswick, Fredericton, NB, Canadá. Es miembro de los Comités ACI 224, Agrietamiento; 435, Deflexión de Estructuras de Construcción en Concreto; 440, Refuerzo de Polímero Reforzado con Fibra; y 440C, FRP Código de Construcción en Concreto Reforzado. Recibió el Reconocimiento de Diseño ACI en 2014, ASCE T.Y. Reconocimiento Lin en 2020 por un trabajo de ACI Structural Journal relacionado con la deflexión del concreto presforzado y el Reconocimiento ACI Symposium Volumes en 2025. Sus intereses de investigación incluyen el comportamiento de capacidad de servicio de las estructuras de concreto.

Wassim Nasreddine es miembro de ACI y Asociado de Investigación en Rutgers, La Universidad Estatal de Nueva Jersey, New Brunswick, NJ, Estados Unidos de Norteamérica. Es miembro de los Comités ACI 435, Deflexión de Estructuras de Construcción en Concreto y 440, Refuerzo de Polímero Reforzado con Fibra. Recibió el Reconocimiento ACI Symposium Volumes en 2025. Sus intereses de investigación incluyen comportamiento de miembros de concreto presforzado, materiales de concreto innovadores y reforzamiento y reacondicionamiento de estructuras de concreto.

Hani Nassif, FACI, es Catedrático de ingeniería estructural en Rutgers. La Universidad Estatal de Nueva Jersey. Es ex miembro del Comité de Actividades Técnicas de ACI (TAC); Jefe del Comité ACI 549, Productos Cementicios Delgados Reforzados y Ferrocemento; Vicepresidente del Subcomité ACI 440-I, Concreto Presforzado FRP; y es miembro de los Comités ACI 209, Fluencia y Contracción en Concreto; 343, Diseño de Puentes de Concreto; 348, Confiabilidad y Seguridad Estructural; 435, Deflexión de Estructuras de Conctrucción en Concreto; 440, Refuerzo de Polímero Reforzado con Fibra; y 444, Monitoreo de la Salud Estructural. Recibió los Reconocimientos Arthur J. Boase y el ACI Symposium Volumes, ambos en 2025. Su investigación se centra en concreto estructural y en el uso de materiales cementicios y compuestos avanzados.

Título original en inglés:

Computing Deflections Using ACI Code-318-19 and Beyond, Part 5

Proposed extension to prestressed concrete

La traducción de este artículo correspondió al Capítulo Centro y Sur de México

Traductora:
Lic. Ana P. García Medina

Revisión Técnica:
Dr. Esteban Astudillo de la Vega